Assessment of mesoporous silica nanoparticle interactions with biofilms by confocal microscopy and surface plasmon resonance

Ronja Hellman 37903

rhellman@abo.fi

Advisors: Anna Slita & Prakirth Govardhanam

Supervisors: Jessica Rosenholm & Tapani Viitala

Pharmaceutical Sciences

Faculty of Science and Engineering

Åbo Akademi University

Åbo, Finland 2022

Abstract

Antibiotic resistance is one of the greater threats to worldwide health today. Misuse and overuse of antibiotic agents puts an evolutionary pressure on bacteria, and several different mechanisms of resistance have been detected. The formation of biofilms, clusters of bacteria protected by an extracellular matrix, is one way for bacteria to protect themselves from antimicrobial agents. The ability to penetrate the extracellular matrix is, therefore, essential for the therapeutic efficacy of antibiotics. Nanoparticles hold potential as an anti-biofilm delivery system, as their small size allows them to pass through biological membranes. The morphology and porosity of mesoporous silica particles are promising for drug-loading and specific targeting of biofilms. The shape, size and surface charge of mesoporous silica particles can be tuned, which offers options for drug-loading as well as biocompatibility. One problem with developing anti-biofilm agents is the lack of *in vitro* models able to represent the complexity of biofilms and their life cycle. Surface plasmon resonance is a relatively new method in biofilm testing but shows great potential as it allows for highly sensitive measurements in real time. In this study, differently shaped and charged mesoporous silica nanoparticles were evaluated for their effect on and penetration of *Staphylococcus aureus* and *Escherichia coli* biofilms. Surface plasmon resonance was evaluated as a method for *E. coli* biofilm testing.

Abbreviations

4Qs	4-quinolone systems
AHL	N-acyl-homoserine lactone
AMPs	Antimicrobial peptides
APTES	Aminopropyl triethoxysilane
BAPs	Biofilm-associated proteins
BSA	Bovine serum albumin
CLSM	Confocal laser scanning microscopy
CMC	Critical micelle concentration
CTAB	Cetyltrimethylammonium bromide
DLS	Dynamic Light Scattering
eDNA	Extracellular DNA
EPS	Extracellular polymeric substances
FITC	Fluorescein isothiocyanate
LB	Luria-Bertani
LD50	Lethal dose 50 %
MSCRAMMs	Microbial surface components recognizing adhesive matrix molecules
MSNs	Mesoporous silica nanoparticles
MSP	Mesoporous silica particles (spheres)
MSR	Mesoporous silica rods
PAP	Peak angular position
PBS	Phosphate buffered saline
PDI	Polydispersity index
PEI	Polyethylenimine
PIA	Polysaccharide intercellular adhesin
PMI	Peak minimum angle
PNAG	Poly-*N*-acetylglucosamine
QS	Quorum sensing

QSI	Quorum sensing inhibitor
RIP	RNAIII-inhibiting peptide
ROS	Reactive oxygen species
SD	Standard deviation
SPR	Surface plasmon resonance
SPRi	Surface plasmon resonance imaging
TEM	Transmission electron microscopy
TIR	Total internal reflection
TSB	Tryptic soy broth

Table of contents

Introduction

Currently, anti-pathogenic agents (primarily antibiotics) are the only viable option for treating infectious microorganisms (Slowing *et al*., 2007). However, adverse side effects, poor solubility and drug resistance are all threats to the future therapeutic efficacy of these agents. In fact, the World Health Organization (2018) defines antibiotic resistance as one of the largest threats to global health. Resistant strains of bacteria are evolved through selective pressure posed by antimicrobial agents and are accelerated by the overuse and misuse of antimicrobial agents. Antibiotic resistance may force a need for high dose administration of antibiotics, with a higher risk of adverse side effects, increased economic cost and prolonged hospitalization time (Chellat, Raguž & Riedl, 2016).

The National Institute of Health (2002) considers 80% of human microbial infections to be associated with biofilms. According to Ceri *et al.* (1999), bacteria in biofilms can be up to a thousand times more tolerant to antimicrobials than bacteria in the planktonic state. Conventional antimicrobial agents have limited effect on biofilms due to poor penetration and weakened effect in the acidic environment of the biofilm matrix (Wu *et al*., 2019). Biofilm-associated microorganisms have been connected to several health issues, such as cystic fibrosis, otitis media, periodontitis, and chronic prostatitis (Donlan, 2002). Furthermore, several medical devices, such as central venous catheters, endotracheal tubes, mechanical heart valves, pacemakers, peritoneal dialysis catheters, prosthetic joints and urinary catheters have been shown to harbor biofilms (Donlan, 2001). Biofilm formation may, therefore, be widely connected to antibiotic resistance in patients with a need for medical devices or with a compromised immune system.

Nanoparticles are defined as ultrafine particles with sizes in the nanometer scale (Hosokawa 2012). The size requirements of particles to be defined as nanoparticles differ depending on the material, but generally a diameter range of 1 to 100 nm is applied. The fine size of the particles allows for easy absorption through biological membranes, as well as increased cellular penetration. Nanoparticles have also shown an increased penetration of biofilms, showing potential as a drug delivery system. For example, Rosemary, Maclaren and Pradeep (2006) showed that ciprofloxacin encapsulated in gold-silica nanoshells improved antibacterial efficiency against *E. Coli*. It was suggested that the shells followed a different route of penetration compared to the free drug, and transmission electron microscopy

showed that the shells were able to enter the bacterial cell. Therefore, nanoantibiotics could be an important tool in overcoming antibiotic resistance.

The surface plasmon resonance (SPR) biosensor provides highly sensitive measurements of kinetics and affinity of bimolecular interactions in real time (Singh, 2016). It has been used in the fields of biological studies, health science research, drug discovery, clinical diagnosis, and environmental and agricultural monitoring. While the utilization of SPR for studying biofilms is relatively new, it holds promise as it provides label-free quantitative assessment of biofilm dynamics on large channel surfaces up to 1 cm^2 (Abadian *et al*., 2014). The real-time measurement can track each stage of the biofilm life cycle, which is essential for developing anti-biofilm agents.

1 Biofilms

Biofilms can be characterized as hydrated surface-associated communities of bacteria encased in an extracellular matrix (Stewart & Frankling, 2008). Biofilms can form on a range of biotic and abiotic surfaces and are present in essentially every part of the human body where bacteria can be found (Karatan & Watnick, 2009). In fact, it has been estimated that only 0.1% of the total microbial mass on earth is in a planktonic mode of growth, and the majority is instead in a form of aggregative state (Bjarnsholt *et al*., 2013). The physiological properties of biofilms differ vastly from bacteria in the planktonic state. The main component of the biofilm is not the bacteria themself but the extracellular matrix, which makes up 90% of the dry mass (Flemming & Wingender, 2010). The matrix consists of extracellular polymeric substances (EPS) which enable the unique qualities of biofilms. The EPS acts as a protective barrier for the bacteria and accounts for the adhesion of biofilms to surfaces, the mechanical stability of biofilms and water retention. The water phase of the matrix contains nutrients and preserved components of dead cells, including DNA, providing the biofilm with a genetic archive.

1.1 Biofilm formation

Biofilm formation can be described as a two-stage process, where the first stage is adherence of bacteria to a surface (adhesion stage), and the second stage is proliferation and differentiation of the attached cells (maturation stage) (Chen & Wen, 2011). Adhesion is the

most critical part as adherence to a surface is essential for biofilm formation. After attachment, the cells will start to divide and extracellular substances will be produced, forming a biofilm (figure 1). In the maturation stage the biofilm grows from a thin layer to a thick mushroom shaped structure (Rabin *et al.*, 2015). The final stage of the biofilm lifecycle is dispersion, where bacteria return to the planktonic stage and migrate to new areas (Petrova & Sauer, 2016). Understanding the biofilm formation process is essential for the development of anti-biofilm agents, as the resistance to antibiotics has been shown to increase with increasing age of the biofilm (Singla, Harjai & Chhibber, 2013).

1.1.1 Adhesion stage

Biofilms can form on almost any surface in natural, industrial and medical settings (López, Vlamakis & Kolter, 2010). Surface properties will affect both the attachment and the formation of the biofilm. Generally, rough surfaces with a high surface area show an increase in microbial colonization (Donlan 2002). Bacteria will also attach more rapidly to hydrophobic, nonpolar surfaces, such as plastics, than to hydrophilic materials, such as glass or metal (Fletcher & Loeb, 1979). Characteristics related to the aqueous medium, such as flow velocity, pH, nutrient levels and temperature, also play a role (Donlan, 2002).

Attachment to a surface occurs in two stages: reversible and irreversible attachment (Petrova & Sauer, 2016). Reversible attachment is usually mediated through hydrophobic interactions and is very unstable, often leading to bacteria detaching and returning to the planktonic stage. Hydrophobic interactions tend to increase with increasing nonpolar nature of the surfaces involved, so the hydrophobicity of the bacterial cell as well as the surface is important in initial attachment. The irreversible attachment which is more stable often involves surface proteins. For example, *P. fluorescens* is dependent on the lipopolysaccharide assembly protein A (LapA) surface protein to go from the reversible to the irreversible stage of attachment (Hinsa *et al.,* 2003). Surface structures, such as fimbriae, flagella and pili, also play a role (Bullitt & Makowski 1995; Korber *et al.*, 1989; Donlan 2002). For example, *E. coli* uses Type I fimbriae for adherence to epithelial cells during urinary tract infections (Wright, Seed & Hultgren, 2007). Staphylococci use a group of adhesion protein called microbial surface components recognizing adhesive matrix molecules (MSCRAMMs) to adhere to the extracellular matrix of host cells (Patti *et al*., 1994). Cell bound polysaccharides can also assist in attachment. For example, Polymeric β-

1,6-*N*-acetyl-D-glucosamine participate in *E. coli* and *S. epidermidis* biofilm adhesion (Itoh *et al*., 2005).

1.1.2 Maturation stage

If the conditions are right, the bacterial cells will start to divide and form a biofilm after attachment. With *S. aureus*, attachment was shown to happen within the first hour of introducing planktonic bacteria to a surface, followed by an active maturation stage for up to five hours, and reaching a plateau phase after six hours (Fallarero *et al*., 2013). The plateau phase is characterized by decreased metabolic activity. With *P. aeruginosa*, the plateau phase was reached after 72 hours of incubation, showing maximum density and bacterial count (Shafique *et al*., 2017). After the fifth day, a decline in density was seen. Similar results were obtained by Anwar, Strap and Costerton (1992), where *P. aeruginosa* biofilms older than five days showed higher resistance to tobramycin and piperacillin compared to younger biofilms. Fouladkhah, Geornaras and Sofos (2013) studied seven strains of pathogenic *E. coli* and found that all expressed a similar increase in bacterial count over a period as long as seven days. In a study by Reisner *et al.* (2003), *E. coli* was shown to form irreversible attachment within two hours in flow-chambers. After 11 hours of development, the cells were distributed evenly over the surface as single cells or pairs of two. After 20 hours a loose, irregularly shaped meshwork had formed and most of the cells were no longer in contact with the surface. After 36 hours, the biofilm thickness had increased tenfold from 7 mm to 70 mm. After 42 hours, the biofilm exhibited higher density and enhanced stability to flow. Lüdecke *et al.* (2014) showed similar results when growing *E. coli* on a titanium oxide surface. SEM images showed initial attachment of single cells to the surface after 24 hours, formation of microcolonies after 48 hours, early biofilm formed after 3 days and height and biomaterial surface coverage increasing over days 3 to 6.

1.1.2.1 Quorum sensing

In the maturing stage of biofilm formation, Quorum sensing systems (QS) play a critical role by regulating cell differentiation and development of biofilm structures (Chen & Wen, 2011). QS is a communication system between bacterial cells where individual cells produce and release small QS signaling molecules and detect the signal in the surrounding environment at the same time. When the hormone-like signaling compounds reach a certain concentration, they interact with bacterial transcriptional regulators of target genes (Sperandio, Torres & Kaper, 2002). Several QS systems have been identified. N-acyl-

homoserine lactone (AHL) systems have been studied in strains of gram-negative bacteria, such as *P. aeruginosa* and *P. putida*, and is believed to regulate biofilm formation (Schuster *et al*., 2003; Bertani & Venturi, 2004). Another signaling system used by *P. aeruginosa* is the hydrophobic 4-quinolone systems (4Qs). 4Qs influence biofilm development and cellular fitness, and is also not restricted to *P. aeruginosa*, suggesting communication with other related bacterial species in multispecies biofilms (Diggle *et al*., 2006). AgrD peptide systems have been shown to be critical for biofilm formation in *L. monocytogenes* (Riedel *et al*., 2009). A deletion mutation in the structural gene for the AgrD peptide showed reduced biofilm formation as well as decreased virulence in mice. The LuxS quorum-sensing system has also been connected to virulence in *V. vulnificus* (Kim *et al*., 2003). Therefore, targeting the specific QS system of a bacterial species holds potential as a way to prevent biofilm formation.

1.1.3 Dispersion

The final stage of the biofilm formation is dispersion, where single cells are released from the biofilm to resume a planktonic lifestyle. The release of bacteria from a biofilm can happen through desorption, detachment, and dispersion (Petrova & Sauer, 2016). The different ways for bacteria to leave the biofilm are shown in figure 1. Desorption usually happens in the early stages of biofilm formation, as a reversion of the bacterial attachment process. Detachment can happen through erosion (continuous removal of biomass) or sloughing (removal of intact pieces of biofilm). In dispersion, single motile bacteria escapes through holes in the microcolony wall. Desorption and detachment are passive processes, while dispersion is an active and regulated process of releasing bacteria from the biofilm.

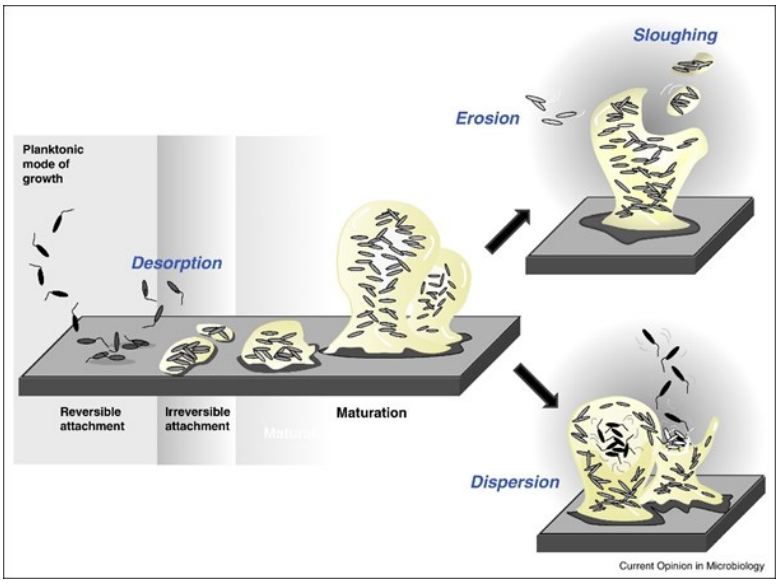

Figure 1. The biofilm life cycle and the different ways bacteria can leave the biofilm; Desorption, detachment (erosion or sloughing) and dispersion (Petrova & Sauer, 2016).

As the planktonic stage is generally considered the more vulnerable stage, certain triggers are needed to induce the dispersion of the biofilm. These triggers can be divided into native and environmental induces (Rumbaugh & Sauer, 2020). Native inducers include response signals to grades of nutrients and oxygen as well as extracellular signaling molecules. Gjermansen *et al.* (2005) showed rapid dissolution of entire *P. putida* biofilms when subjected to carbon starvation. Genetic analysis suggested that the genes PP0164 and PP0165 played a role in the dissolution of the biofilm. In *P. aeruginosa*, the signaling compound cis-2-decenoic acid has been directly linked to dispersion (Davies ja Marques 2009). Environmental inducers include NO, cis-DA, iron, and a step-increase of various nutrients including sugars and amino acids (Rumbaugh & Sauer, 2020).

1.2 Extracellular matrix

The cell secreted extracellular polymeric substances (EPS) make up the majority of the biofilm structure (Donlan, 2002). Its physical and chemical properties vary not only based on the species, but also the environment it grows in. The primary component of the EPS is polysaccharides. The EPS also contain a wide variety of proteins, glycoproteins and glycolipids (Flemming, Neu & Wozniak., 2007). The EPS is highly hydrated and can incorporate large amounts of water into its structure by hydrogen bonding. In fact, as much as 97% of the extracellular matrix can consist of water (Zhang, Bishop & Kupferle, 1998).

Some biofilms have also been found to contain water channels that help in the distribution of nutrients and oxygen (Stoodley, Debeer & Lewandowski, 1994).

1.2.1 Polysaccharides

The composition and structure of the polysaccharides determine many primary properties of the biofilm, such as viscoelasticity and stability. For example, EPS containing 1,3- or 1,4-β-linked hexose residues tend to be more rigid and less soluble (Sutherland, 2001). The stability of the extracellular matrix will depend on the polysaccharide concentration, the ionic strength and the other macromolecules present. The solubility of the polysaccharides may affect the detachment and dispersal of biofilm material. Several biofilm polysaccharides have been identified. In *S. typhimurium* and *E. coli* cellulose has, together with thin aggregative fimbriae, been shown to be a crucial component of the extracellular matrix (Zogaj *et al*., 2001). This composition leads to a highly hydrophobic and rigid matrix. Staphylococcal polysaccharide intercellular adhesin (PIA) or the related poly-N-acetyl glucosamine (PNAG) polymer play a role in adhesion of biofilms to surfaces as well as mediating accumulation of cells into biofilms (Maira-Litran *et al.,* 2002). PIA-like polymers seem to be produced by several Gram-negative bacterial species (Branda *et al*., 2005). For example, Wang, Preston & Romeo (2004) suggested that the PIA-like polysaccharide β-1,6-N-acetyl-d-glucosamine works as an adhesin that stabilizes biofilms of *E. coli* and other bacteria.

What makes the extracellular matrix complex is that individual strains are often able to produce several different extracellular polysaccharides (Branda *et al*., 2005). For example, *P. aeruginosa* makes biofilms by producing three different exopolysaccharides: alginate, Pel, and Psl (Colvin *et al*., 2012). Overproduction of alginate characterizes mucoid strains, while non-mucoid strains use either Pel or Psl as the primary matrix structural polysaccharide. Psl also plays an important role in surface attachment. The composition of polysaccharides has been shown to vary greatly within biofilms. Leriche, Briandet & Carpentier (2003) showed that different organisms produce differing amounts of EPS. The amounts of EPS were also higher in 4-day biofilms than in 1-day biofilms for the majority of the strains tested.

1.2.2 Proteins

Biofilm-associated proteins (BAPs) is the common name for a group of surface proteins with similar structural and functional features (Lasa & Penadés, 2006). The characteristic qualities of BAPs are a high molecular weight, presence on the bacterial surface, a core domain of tandem repeats, involvement in biofilm formation and in bacterial infectious processes. A list of BAPs can be seen in table 1. For example, the surface protein BapA is a crucial mechanical component of *Salmonella* biofilms as well as involved in *Salmonella* invasion (Guttula *et al*., 2019). Another group of biofilm proteins are amyloid proteins, which are able to form organized deposits of thin needle-like structures called amyloid fibers (Dueholm *et al*., 2010). The enterococcal curli is one of the most studied amyloid proteins, and is involved in adhesion to surfaces, cell aggregation and biofilm formation (Barnhart & Chapman, 2006). A similar structure is found in *Salmonella*, called Tafi or thin aggregative fimbriae (Collinson *et al*., 1991). In *S. mutans*, Glucan-binding proteins (for example P1) were shown to be essential for biofilm growth, and in the absent of these proteins the developed biofilm was significantly thinner (Lynch *et al*., 2007). The protein Bap in *S. aureus* has been shown to have a dual function, first working as a sensor on the cell surface and later able to form amyloid scaffold structures to promote biofilm development under specific environmental conditions (Taglialegna *et al*., 2016). Most biofilms will contain a range of different proteins. For example, Piras *et al*., (2021) found 14 different proteins produced by *S. aureus* strains, three of which were specific to the high biofilm-producing strains (alcohol dehydrogenase, ATP-dependent 6-phosphofructokinase and fructose-bisphosphate aldolase).

Table 1 Biofilm related proteins and their function.

Protein	**Characteristics**	**Bacteria**	**Function**	**Reference**
Curli	Amyloid protein	*E. coli*	Adhesion to surfaces, cell aggregation and biofilm formation	Barnhart & Chapman, 2016
Tafi	Amyloid protein	*Salmonella*	Adhesion to eukaryotic cells and biofilm formation	Collinson *et al*., 1991
MTP (pili)	Amyloid protein	*M. tuberculosis*	Biofilm formation	Ramsugit *et al*., 2013

Fap	Amyloid protein	*Pseudomonas sp.*	Structural biofilm matrix molecule	Dueholm *et al*., 2010
TasA	Amyloid protein	*B. subtilis*	Structural biofilm matrix molecule	Romero *et al*., 2010
P1	Amyloid protein	*M. streptococci*	Structural biofilm matrix molecule	Oli *et al*., 2012
WapA	Amyloid protein	*M. streptococci*	Cell-wall associated	Barran-Berdon *et al*., 2020
Smu_63c	Amyloid protein	*M. streptococci*	Biofilm development, regulator of genetic competence and biofilm cell density	Barran-Berdon *et al*., 2020
PSMs	Amyloid protein	*S. aureus*	Biofilm integrity	Schwartz *et al*., 2012
Tu Elonga-tion factor	Amyloid protein	*G. anatis*	Adhesion during biofilm formation	López-Ochoa *et al*., 2017
Bap	BAP Amyloid protein	*S. aureus*	Early adherence, intercellular adhesion and biofilm formation	Cucarella *et al*., 2001
BapA	BAP	*Salmonella*	Adhesion, mechanical component and involved in invasion	Guttula *et al*., 2019
Bhp	BAP	*S. epidermidis*	Biofilm formation	Trotonda *et al*., 2005; Lasa & Penadés, 2006
Esp	BAP	*E. faecalis*	Biofilm formation	Toledo-Arana *et al*., 2001
LapA	BAP	*P. fluorescens*	Biofilm formation	Hinsa *et al*., 2003
Esp	BAP	*E. faecium*	Adhesion to eukaryotic cells	Lund & Edlund, 2003
Lsp	BAP	*L. reuteri*	Adherence to epithelial cells and biofilm formation	Walter *et al*., 2005
YeeJ	BAP	*E. coli*	Biofilm formation	Roux, Beloin & Ghigo, 2005

Proteins can have other functions critical for biofilm formation. TapA is a protein with a disordered structure that mediates the assembly of the amyloid protein TasA into fibers and anchors these fibers to the cell surface (Abbasi *et al*., 2018). Zhang *et al.* (2020) found that the protein YmdB was critical for the biofilm formation of a strain of *B. cereus*, as deletion of the protein encoding gene reduced the ability to form complex spatial structures. YmdB was suggested to have a regulatory effect on mobility, enabling biofilm formation as it would be impossible with freely moving cells. Ryan *et al.* (2009) found that HD-GYP domain proteins regulate motility, virulence and biofilm architecture of *P. aeruginosa*, as mutations in these proteins led to a reduction in motility and a reduction in bacterial virulence in the larvae of *G. mellonella*. In *B. subtilis*, the protein BslA forms a hydrophobic, elastic surface layer around the biofilm, which acts as a protective layer against mechanical forces (Hobley *et al*., 2013; Liu *et al*., 2017). Branda *et al.* (2006) showed that *B. subtilis* biofilm formation was dependent on both an amyloid-like protein component, TasA, and an exopolysaccharide component. Interestingly, the biofilm was successfully grown even when TasA and the exopolysaccharide were produced by different cells, confirming matrix formation as an extracellular process. Identifying proteins critical to the formation and survival of biofilms could be a method of fighting biofilm related infections.

1.2.3 Extracellular DNA

In addition to polysaccharides and proteins, extracellular DNA (eDNA) contributes to the structural integrity of biofilms. eDNA is involved in the initial stage of adhesion, acts as a structural component and promotes biofilm aggregation (Whitchurch *et al*., 2002; Rice *et al*., 2007; Izano *et al*., 2008). In *S. Aureus*, mutation of the *cidA* gene led to the biofilm being less adherent as well as a decrease in cell lysis and release of eDNA (Rice *et al*., 2007). This suggests that *cidA*-controlled cell lysis plays an important role during biofilm development and that released eDNA is an important structural component of the *S. aureus* biofilm. Whitchurch *et al*. (2002) found that addition of the DNA degrading DNase enzyme not only inhibited *P. aeruginosa* biofilm formation, but also dissolved the biofilm in early stages of formation. This indicates that eDNA is required for the initial establishment of *P. aeruginosa*. The eDNA was speculated to be derived from membrane vesicles, as cell lysis didn't seem to be occurring during biofilm formation. Similar results were obtained when treating *L. monocytogenes* with DNase I, where the success of attachment and adhesion

seemed to be linked specifically to high-molecular-weight DNA (Harmsen *et al*., 2010). It was suggested that this DNA together with N-acetylglucosamine could form a polymer with properties resembling those of PNAG of *Staphylococcus* and *E. coli*. In a study by Izano *et al*. (2008) of *S. aureus* and *S. epidermidis* biofilms, *S. aureus* biofilms were detached by addition of DNase I but *S. epidermidis* was not. On the other hand, *S. epidermidis* biofilms were detached by the addition of PNAG-degrading enzyme dispersin B while *S. aureus* biofilms were unaffected. Even though eDNA is a structural component in both biofilm matrixes, it seems to have varying grades of importance in different strains.

1.3 Resistance to antibiotic agents

Several mechanisms have been proposed to explain the high resistance of biofilms to antibiotics. It is generally assumed that the extracellular matrix acts as a protective barrier separating the cells from the surrounding environment (Mah & O'Toole, 2001). Restricted penetration of antimicrobial agents into the biofilm has been suggested to limit their efficacy, although other mechanisms of reduced biofilm susceptibility seem to be present (Stewart, 1996).

1.3.1 Biological heterogenicity

The biological heterogeneity of biofilms has been suggested as a method of resistance (Stewart & Franklin, 2008). The environmental conditions within the biofilm vary regarding oxygen levels, concentration of nutrients, signaling compounds and bacterial waste. As the bacteria respond and adapt to the local environment, the cells in the biofilm will vary from each other both spatially and temporally as the biofilm develops. When cells go from rapid to slow or no growth, it is generally accompanied by an increase in resistance to antibiotics (Mah & O'Toole, 2001). Borriello *et al*. (2004) showed that most of the cells in P. *aeruginosa* biofilms were in an oxygen-limited, stationary-phase state after 48 hours of growth, and showed a lower sensitivity to antibiotics. Additionally, after 4 hours when the biofilms were still actively growing, biofilms under anaerobic conditions showed reduced sensitivity to antibiotics compared to controls grown aerobically. This suggests that local oxygen limitation may contribute to the antibiotic susceptibility of *P. aeruginosa* biofilms. Different levels of nutrients will also affect the susceptibility to antibiotics. Nguyen *et al*. (2011) showed that *P. aeruginosa* biofilms grown in a nutrient-limited environment showed higher

resistance to antimicrobial agents. The protective mechanism seemed to be due to an active response to starvation linked to reduced levels of oxidative stress in the cells.

1.3.2 Genetic variation

The confined space of the EPS matrix leads to constant competition and adaptation of population fitness (Flemming & Wingender, 2010). While the chemical heterogeneity and physiological adaptation to the local environment is the major contributor to the heterogeneity in biofilms, genetic variation may also be present. This can be observed primarily as changes in the colony morphology of subpopulations of cells. For example, morphological variants of *S. pneumoniae* show differences in colony diameter, mucoid levels, auto-aggregation, initial attachment, hydrophobicity, capsule production and biofilm formation (Allegrucci & Sauer, 2007). *P. aeruginosa* shows small, rough, strongly cohesive colony morphology variants (Kirisits *et al*., 2005). In addition, bacterial cells in a biofilm may show stochastic gene expression that generates phenotypic diversity independent of the environmental conditions (Stewart & Franklin, 2008). One phenotypic resistance that has been suggested is the expression of efflux pumps that can extrude chemically unrelated antimicrobial agents from the cell (Mah & O'Toole, 2001). Another theory is the expression of genes involved in the general stress response. The *rpoS* gene has been connected to biofilm formation, and the *rpoS*-mediated stress response has been linked to antibiotic resistance (Adams & McLean, 1999; Mah & O'Toole, 2001). Although several mechanisms and genes have been proposed, it is likely that a combination of different mechanisms account for the biofilm resistance to antibiotics (Ito *et al*., 2009).

1.3.3 Multispecies biofilms

When studying biofilm resistance, most studies focus on monospecies cultures. However, nearly all biofilms in nature consist of a variety of microorganisms (Elias & Banin, 2012). Multispecies biofilms are also prominent in the human host, for example in oral biofilms and in cases of cystic fibrosis (Jakubovics, & Kolenbrander, 2010; Woods *et al*., 2018). While some bacteria will compete when occupying the same space and using the same nutritional resources, beneficial cooperation between different species of bacteria has been identified. One example is the attachment to a surface. Leung *et al.* (1998) showed that pre-colonization with *E. coli* would facilitate later attachment of *Enterococcus*. *S. gordonii* has also been shown to express genes specifically to recruit *Porphyromonas gingivalis* into

mixed species biofilms (Kuboniwa *et al*., 2006). Some bacteria have shown metabolic cooperation in mixed species biofilms. This was shown in a study by Christensen *et al*. (2002) where *P. putida* in the presence of *Acinetobacter* will metabolize benzoate produced by *Acinetobacter* as an energy source. This cooperation can be seen in the structure of the biofilm, as *Acinetobacter* will reside in the upper layers of the biofilm close to the nutrient source and *P. putida* resides in the lower layers benefiting from the benzoate produced. Another synergistic relation is the cohabitation of anaerobic and aerobic bacteria in aerobic conditions. The anaerobic bacteria are able to survive because the aerobic bacteria will consume the oxygen and provide anaerobic conditions in the deeper levels of the biofilm (Bradshaw *et al*., 1997). It has been suggested that bacteria living in multispecies biofilms can communicate through quorum sensing. The AI-2 system is used by a range of different species of bacteria and is considered to be involved in interspecies communication (Waters & Bassler, 2005). QS systems have shown importance in the formation of mixed species biofilms, for example the formation of oral biofilm by *P. gingivalis* and *S. gordonii* which is mediated by the AI-2 system (McNab *et al*., 2003).

The cooperation and communication of mixed species biofilm allow the biofilm to grow thicker and survive exposure to the immune system and antimicrobial agents (Al-Bakri, Gilbert & Allison, 2005). Burmølle *et al.* (2006) showed synergistic relations between four epiphytic bacterial strains, isolated from the surface of marine alga. The biomass of the biofilms was increased by over 167% compared to single species biofilms and showed higher resistance to antimicrobial agents (hydrogen peroxide or tetracycline). Leriche, Briandet & Carpentier (2003) showed that *S. sciuri* when grown together with a strain of *Kocuria* showed higher susceptibility to an alkaline chlorine solution. In the presence of chlorine, *S. sciuri* cells were distributed as a ring around *Kocuria* microcolonies. This suggests a protective mechanism of *S. sciuri* for this strain of *Kocuria*. Multispecies biofilms also show higher resistance to the immune response. In a study by Ramsey & Whiteley (2009), cocultivation of two oral bacteria, *S. gordonii* and *A. actinomycetemcomitans*, showed enhanced resistance to killing by host immunity. The resistance was explained by *S. gordonii* producing the streptococcal metabolite hydrogen peroxide, to which *A. actinomycetemcomitans* can react by enhancing expression of the resistance protein ApiA.

The cohabitation of bacteria has been shown to have clinical importance. In a study by Al-Bakri, Gilbert & Allison (2005), *P. aeruginosa* and *B. cepacian* from a cystic fibrosis patient formed highly resistant biofilms not susceptible to tobramycin or gentamicin. Another pair

of bacteria often present in cystic fibrosis infections is *S. aureus* and *P. aeruginosa*. Hoffman *et al*. (2006) showed that when cocultured, *S. aureus* respiration is suppressed by a *P. aeruginosa* exoproduct, increasing its resistance to aminoglycoside antibiotics, such as tobramycin. The resistance was explained by *S. aureus* selectively growing in small-colony variants, known for their ability to evade the host immune defense, and their higher susceptibility to antimicrobial agents (Samuelsen *et al*., 2005). Understanding the mechanisms of cohabitation in mixed species biofilms is necessary for understanding their enhanced antibiotic resistance.

1.4 Treatment options for biofilms

The complexity and variety of biofilms create a need for new antimicrobial treatment methods. To this day, there are no biofilm-specific drugs available for human applications (Verma *et al*., 2022). Antimicrobial agents, while they may be used to kill the bacteria, can still leave behind other biofilm components, causing problems, for example, on medical devices (Koo *et al*., 2017). Current treatment methods specifically designed for biofilms include physical-mechanical methods, such as jets and sprays for biofilm disruption or removal, and surface-coating or eluting substrates impregnated with antibiotics and/or antimicrobials. Several antimicrobial metals have also been used to prevent biofilm formation, such as silver coating in catheters and wound dressings, and copper alloys in hospital surfaces (Lemire, Harrison & Turner, 2013). Several anti-biofilm treatment options have been suggested, although most are at an early stage of development and need further studies to determine their efficacy and safety in clinical applications.

1.4.1 Adhesion inhibitors

Adhesion to the surface is a critical step of biofilm formation, making surface proteins a compelling target for anti-biofilm treatments. Hundreds of surface proteins from different microbial species have been identified and suggested as targets for anti-adhesion compounds (Chen & Wen, 2011). However, the variety in surface proteins in different species, as well as the ability for multiple different interactions with different host components, makes targeting a specific protein insufficient. Therefore, focusing on reactions or processes that are shared by most surface proteins is a more valid treatment option. Sortase of Gram-positive bacteria is such a candidate. Sortase are membrane enzymes that catalyze the

covalent attachment of specific proteins to the cell wall (Paterson & Mitchell, 2004). Wang *et al*. (2018) showed that quercetin was able to significantly decrease the catalytic activity of sortase A, leading to a decrease in *S. pneumoniae* biofilm formation and biomass. In a study by Hu, Huang & Chen (2013) curcumin, an active ingredient of turmeric, was showed to have an inhibitory effect on sortase A. The inhibition of the enzymic activity led to a release of the Pac protein to the supernatant and a reduction in *S. mutans* biofilm formation. High-throughput screening has also been used to identify several promising compounds for sortase inhibition, such as diarylacrylonitriles (Cascioferro, Totsika & Schillaci, 2014). However, many of the studies of inhibitors focus on enzymatic models and do not always include further *in vivo* or *in vitro* studies.

Another way of preventing the initial settlement of biofilms is anti-biofilm coatings. Antiadhesive materials have been used in industrial settings to prevent biofilm formation, for example metal complex films, antimicrobial peptides, proteolytic enzymes, and surfactants (Golberg *et al*., 2016; Cloete & Jacobs, 2001). In medical settings, biofilms forming on medical implants, indwelling devices and surgical equipment represent a significant clinical challenge. Grover *et al*. (2016) developed anti-biofilm coatings by immobilizing acylase into polyurethane films. The coating disrupts quorum sensing in surface-associated bacteria, which was followed by inhibition of biofilm formation by *P. aeruginosa*. Sae-ung *et al*. (2019) developed a universal coating of an antifouling polymer that could inhibit adhesion of bacteria on medical implants, catheters, or endotracheal tubes. The coating contains methacryloyloxyethyl phosphorylcholine that provides the antifouling property, and a methacrylate-substituted dihydrolipoic acid that offers cross-linkable sites via thiol-ene reactions to achieve robust thin films. Although a proactive prevention of biofilm formation would be efficient, such methods are usually limited by effect duration as well as the inability to differ between short-term biocidal activity and long-term biofilm inhibition (Grover *et al*., 2016).

1.4.2 Quorum sensing inhibitors

As QS is an important part of the maturation stage of the biofilm, quorum sensing inhibitors (QSI) may keep the bacteria in a planktonic stage. The naturally produced plant metabolites called flavonoids have been extensively studied as QSI. Flavonoids have been shown to inhibit quorum sensing via antagonism of the autoinducer binding receptors, LasR and RhlR (Paczkowski *et al*., 2017). In a study by Wu *et al*. (2004), two synthetic furanones were

tested in a mouse model of chronic lung infection by *P. aeruginosa*. Furanones showed accelerated lung bacterial clearance, reduction of the severity of lung pathology and prolonged survival time of the mice in lethal infections. The RNAIII-inhibiting peptide (RIP) is another promising QSI. RIP inhibits quorum-sensing mechanisms by inhibiting the phosphorylation of the *trp* RNA-binding attenuation protein (TRAP) (Balaban *et al*., 2007). Balaban *et al*. (2003) showed that RIP combined with antibiotics was successful in eliminating 100% of graft-associated *in vivo S. epidermidis* infections. Similar results have been shown for *S. aureus* graft infections, where rats treated with RIP showed a significant reduction of biofilm mass (Balaban *et al.,* 2007). Despite promising results in animal models, the clinical application of RIP may be problematic due to product stability and toxicity of the peptide drug (Chen & Wen, 2011).

1.4.3 Antimicrobial peptides

Antimicrobial peptides (AMPs) can be used as antimicrobial agents due to their ability to bind to structurally important molecules on the microbial membrane (Chen & Wen, 2011). AMPs are widespread in nature, have a broad spectrum of antimicrobial activity, and development of resistance is rare. However, the difficulty and expensive nature of large-scale production as well as their sensitivity to protease digestion has led to the development of synthetic antimicrobial peptides. Eckert *et al*. (2006) developed a synthetic, target-specific antimicrobial peptide, G10KHc, designed to specifically target *Pseudomonas* cells. The peptide showed enhanced killing activities due to increased binding and penetration of the outer cell membrane compared to a generally killing peptide. Multiple-headed antimicrobial peptides have been suggested as a treatment option for polymicrobial infections and removal of biofilm constituents without the use of several distinct molecules. He *et al*. (2009) developed a multiple-headed, target-specific antimicrobial peptide that showed specific activity against *P. aeruginosa* and *S. mutans in vitro*. The peptide was able to remove both species from a mixed planktonic culture with little impact against untargeted bacteria. Such targeted activity shows potential for infection treatment without the negative impact on human normal flora.

1.4.4 Targeting the extracellular matrix

Targeting of the extracellular matrix of biofilms is mainly based on the inactivation of structural components which causes the bacteria to switch back to the planktonic stage. As

mentioned earlier, eDNA has been shown to be a critical structural component in many biofilms. Targeting eDNA is, therefore, a valid treatment method. Hymes *et al*. (2013) showed that treating *G. vaginalis* biofilms with DNase released bacteria from the biofilm and increased the antimicrobial activity of metronidazole. DNase could potentially work as a nonantibiotic adjunct to existing antimicrobial therapies. Extracellular proteins are another potential target. Verma *et al*. (2022) showed inhibition of *B. subtilis* biofilm formation by targeting the major structural protein, $TasA_{(28-261)}$. The inhibitors lovastatin and simvastatin were identified through virtual screening and showed significant results *in vitro* by causing the disintegration of pre-formed biofilms. Olsen *et al*. (2018) combined the endolysin LysK and the poly-N-acetylglucosamine depolymerase DA7 to reduce staphylococcal biofilms. Endolysins work as anti-bacterial agents by degrading the bacterial cell wall, and depolymerases targets polysaccharides in the extracellular matrix. While both components show anti-biofilm efficacy, combined they significantly reduced viable cell counts compared to individual enzyme treatment.

Another way to target the extracellular matrix is the utilization of the dispersion process. Howlin *et al*. (2017) demonstrated the use of low-dose nitric oxide for cystic fibrosis infection treatment in an *ex vivo* model and a proof-of-concept, double-blind clinical trial. Nitric oxide functions as a signaling molecule, inducing biofilm dispersal in *P. aeruginosa* biofilms. In the 12-patient randomized clinical trial, nitric oxide inhalation as an adjunctive therapy to antibiotics caused significant reduction in *P. aeruginosa* biofilm aggregates compared to placebo across 7 days of treatment. Davies ja Marques (2009) found that *P. aeruginosa* produces an organic compound, cis-2-decenoic acid, which is an extracellular messenger involved in the dispersion of the biofilm. When accumulated, the acid will cause increased biofilm dispersion and biofilm eradication. This compound was able to induce dispersion in biofilms formed by a range of different bacteria, such as *E. coli*, *S. pyogenes*, *B. subtilis*, *S. aureus*, and the yeast *Candida albicans*. However, the composition of the extracellular matrix varies greatly depending on the type of microorganism, local mechanical shear forces, substrate availability and the host environment (Koo *et al*., 2017). This, combined with the interactions among the various components, adds complexity to potential EPS targeting anti-biofilm treatments.

2 Nanoantibiotics

Nanoparticles show great potential in overcoming the issues of antibiotic resistance. Compared to traditional antimicrobial agents, a wider range of pathogenic inactivation mechanisms is possible with nanostructures (Jijie *et al*., 2017). Nanoparticles may interact with proteins in the cell wall, causing irreversible changes to the structure and permeability, which impairs the ability of the cells to regulate transport activity and causes leakage of cellular content, such as ions, proteins and ATP. Depending on the size of nanoparticles, they may also penetrate the cell membrane and disrupt intracellular mechanisms, such as mitochondrial function and protein/ribosome stability, or interact directly with the DNA of the cell. Another mode of action is causing cellular toxicity through an increase in oxidative stress by generating reactive oxygen species (ROS), such as hydrogen peroxide.

Nanoantibiotics, aka antibiotic loaded nanoparticles, have shown significant advantages compared to free antimicrobial agents. As a delivery system, nanoparticles provide targeted drug delivery via specific accumulation and, therefore, fewer side effects. Drug release can be controlled, and the elimination time is longer, which leads to extended therapeutic lifetime. Importantly, the solubility of the drug can be improved, which increases the efficacy and reduces side effects (Huh & Kwon, 2011). For example, Nirmala Grace & Pandian (2007) showed that combining antibiotics (streptomycin, gentamycin and neomycin) with gold nanoparticles increased the antibacterial efficiency against strains of both gram-positive and gram-negative bacteria, such as *S. aureus*, *M. luteus*, *E. Coli* and *P. Aeruginosa*. The increased efficiency was explained by favorable alteration of the metabolite pathway and release mechanism. Targeted delivery was also achieved by Wu *et al*. (2019) by biofilm-responsive nanoantibiotics composed of silver nanoclusters, that in the acidic environment of the biofilm would disassemble and allow for penetration of the biofilm and release of toxic silver ions. Improved anti-biofilm activity was shown both *in vitro* and *in vivo*, showing potential for combating resistant bacterial biofilm-associated infections.

2.1 Mesoporous silica nanoparticles

Mesoporous silica nanoparticles (MSNs) are promising inorganic nanomaterials, with desired qualities for drug delivery. These qualities include controllable particle size, morphology (shape), and porosity, as well as chemical stability (Slowing *et al*., 2007). These

properties enable encapsulation of a variety of therapeutic agents and delivery of these agents to the desired location. The large pore volume, surface area and the lack of interconnection between individual porous channels allow for high drug-loading and controlled release kinetics (Zhou *et al*., 2018). The pore volume is usually above 1 cm^3/g. The pore size and orientation are usually determined by the nature of surfactant templates (Tang, Li & Chen, 2012). The particle size can be controlled from 50 to 300 nm, and the surface area is usually above 700 m^2/g (Zhou *et al*., 2018).

MSNs have been successfully loaded with a range of therapeutic agents including pharmaceutical drugs, therapeutic proteins, and genes (Tang, Li, & Chen, 2012). Compared to traditional drug delivery systems, such as polymer nanoparticles or liposomes, MSNs are more flexible, versatile, and robust, and allow for more heterogeneous distribution, higher drug-loading capacity and a more cost-efficient production. Besides drug and gene delivery, mesoporous nanomaterials can be used for a range of different applications, including biosensors for intracellular controlled release and imaging applications (Slowing *et al*., 2007). For future clinical applications, MSNs show large potential since the manufacture process is relatively simple and the cost of production is low (Tang, Li, & Chen, 2012).

Since the first synthesis of mesoporous silica with uniform pore size in the early 1990s, great progress has been made in the synthesis process (Tang, Li & Chen, 2012). Size, morphology, pore size, and pore structure of MSNs can now be controlled through synthesis parameters. The general synthesis process is shown in figure 2. The surfactant, cetyltrimethylammonium bromide (CTAB) will self-aggregate into micelles when the concentration is above the critical micelle concentration (CMC). The silica precursors will form a silica wall around the micelles by condensing around the polar head region. When the template surfactant is removed by solvent extraction, pores are generated. The silanol groups on the surface of silica materials allow for modification of its chemical properties through functionalization (Vallet-Regí, 2006). Dyes for imaging purposes, differently charged functional groups, stimuli-responsive ligands and targeting molecules are examples of possible surface modifications. A range of different morphologies of mesoporous nanoparticles is possible through controlling reaction conditions, such as temperature, pH and surfactant concentration (Wu, Mou & Lin, 2013). Cai *et al*. (2001) produced different sized nanoparticles in the shapes of spheres and rods by varying the molar ratio of CTAB and tetraethyl orthosilicate (TEOS) and controlling the pH using catalysts. Anderson *et al*. (1998) used different concentrations of methanol as a cosolvent to control size, morphology

and pore diameter. The presence of organoalkoxysilane precursors during the co-condensation reaction will also affect the shape of the particles (Huh *et al*., 2003). By changing the precursor or its concentration, spheres, tubes and rods of various dimensions were produced. The shape of the nanoparticles may affect both drug-loading and drug release capability. A study by Chen *et al*. (2012) showed that rod-shaped mesoporous silica nanoparticles had a higher drug-loading capability of ibuprofen than spheres, which was attributed to a higher surface area. However, rods showed a decreased drug release rate, which was explained by length and curvature of the mesopores. Increasing the drug-loading capability could minimize the amount of silica material needed for delivering a therapeutic amount of a drug.

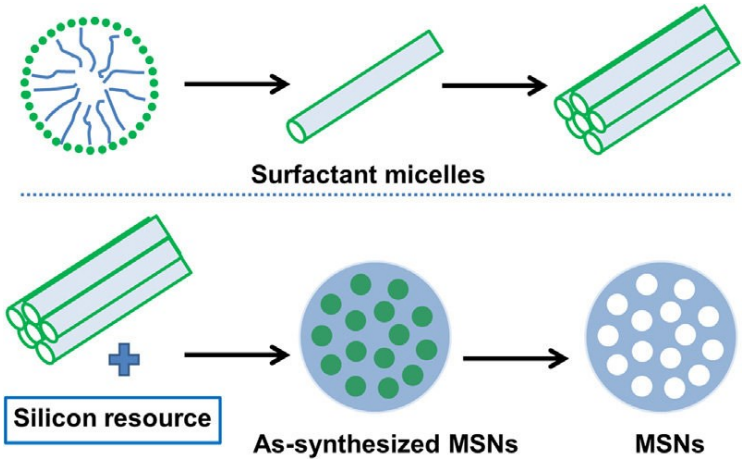

Figure 2. Schematic representation of the synthesis process for mesoporous silica nanoparticles (Zhou et al 2018).

2.1.1 Mesoporous silica particles as nanoantibiotics

Mesoporous silica particles have been successfully loaded with several different antibiotics. In a study by Nairi *et al*. (2017) the adsorption and the release of the antibiotic ampicillin in MCM-41, SBA-15, and SBA-15-NH_2 mesoporous silica materials were investigated. Both loading capacity and release seemed to be greatly dependent on the surface charge density rather than the sorbents morphology. In a study by Sevimli & Yılmaz (2012) amoxicillin was successfully loaded into surface functionalized SBA-15 particles. Although a slightly higher amount of amoxicillin was incorporated, the functionalization did not affect the release profile of amoxicillin. Doadrio *et al*. (2004) achieved controlled release of gentamicin when incorporated in mesoporous silica SBA-15 material in powder and disk forms. *In vitro* studies showed a favorable release profile compared to traditional administration routes where the dissolution is immediate. Tamanna *et al*. (2018) used thin-

film coatings embedded with gentamicin-loaded MSNs to study anti-biofilm activity against *S. aureus* over a prolonged period of time. The anti-biofilm effect remained active for more than 2 months, showing a uniquely slow and controlled release of antibiotic from nanoparticle embedded thin films.

Mesoporous silica nanoparticles can be used as nanocarriers for anti-biofilm agents. Li *et al.* (2016) found that nanoparticle encapsulated chlorhexidine showed enhanced anti-biofilm efficiency compared to the free drug against oral bacterium *S. sobrinus*, *S. mutans*, and *Candida albicans*. The efficiency was explained by the protective effect of the nanoparticles during the penetration of the biopolymer matrix as well as close interaction with microorganisms and an effective releasing mode. Both shapes of nanoparticles used in the study, spheres and wires, were able to penetrate the biofilm. However, the spherical nanoparticle-encapsulated chlorhexidine showed greater anti-biofilm capacity than the wire nanoparticle-encapsulated chlorhexidine. Lu *et al*. (2018) used mesoporous silica nanoparticles to co-deliver silver nanoparticles and chlorhexidine for oral plaque biofilm inhibition. The particles were able to restrict the growth of *S. mutans* biofilms more efficiently and more long-term compared to free chlorhexidine. The particles also showed less cytotoxicity to oral epithelial cells. Álvares *et al*. (2022) developed an advanced nanocarrier system where levofloxacin loaded MSNs were coated with a thermosensitive polymer with the ability to undergo a hydrophilic-to-hydrophobic phase transition at temperatures between 40–43 °C. The surface was decorated with superparamagnetic iron oxide nanoparticles able to generate heat upon application of an alternating magnetic field. The generated heat induces a change in the polymer conformation triggering pore uncapping and antibiotic release. The nanosystem showed a significantly decreased number of viable bacteria in *E. coli* biofilms.

MSNs have also been used to enhance the effect of biofilm eradicating enzymes. Devlin *et al*. (2021) used a combination of MSNs functionalized with enzymes lysostaphin (cell lysis), serrapeptase (protein degradation) or DNase (eDNA degradation) to eradicate *S. aureus* biofilms. The efficacy of all three enzymes was significantly improved when immobilized onto MSNs. The efficacy was further enhanced when all three functionalized MSNs were used as a combination against *S. aureus* biofilms. Tasia *et al*. (2020) successfully loaded silver-doped MSNs with DNase I. The particles showed enhanced antibacterial effects for both Gram-negative *E. coli* biofilms and Gram-positive *S. mutans* biofilms. Overall,

mesoporous silica particles show great potential as a delivery system for antimicrobial agents.

2.1.2 Biocompatibility and toxicity

Silica nanoparticles are generally considered safe, as silica is an abundantly distributed material in nature (Tang, Li, & Chen, 2012). The biocompatibility and toxicity of mesoporous silica nanoparticles can, however, be affected by different physicochemical properties, including particle size, shape, surface area and structure. As far as size is concerned, He *et al*. (2009) concluded that the cytotoxicity of spherical MSNs was highly correlated with particle sizes: particles of the nanoscale (190–420 nm in diameter) showed significant cytotoxicity at concentrations above 25 μg/mL, while microscale particles (1220 nm in diameter) showed slight cytotoxicity over a broad concentration range of 10–480 μg/mL due to decreased endocytosis. Another study by He *et al*. (2011), showed that the biodistributed percentages of both MSNs in liver and spleen increased with an increase of the particle sizes for a short time period. However, both the tested MSNs and PEGylated MSNs showed good tissue compatibility, due to their stable physicochemical properties, biodegradability, and biocompatibility of the particles and the biodegradation products. Additionally, PEGylation of MSNs partially prevented the particles from distributing to the liver, spleen, and lung, which also led to longer blood-circulation lifetime, slower biodegradation, and correspondingly lower levels of degradation products than for the MSNs of the same particle sizes. In fact, surface properties are considered one of the most important aspects of nanoparticles biocompatibility after size (Tang, Li, & Chen, 2012). For example, nanoparticles with a cationic charge can cause cytotoxicity by compromising the integrity of the cell membrane (Nel *et al*., 2009). Another example is exposed surface silanol groups that can interact with biological molecules, for example cellular membrane lipids and proteins, and destroy the structure of these molecules. PEGylation is one method of overcoming this problem (Slowing *et al*., 2009).

The biodistribution, clearance, and biocompatibility of nanoparticles can also be linked to the shape of the particles. However, studying this might be a challenge as it requires MSNs of different shape but similar composition, structure, diameter, and dispersity (Tang, Li, & Chen, 2012). An example of the effect of the shape is shown in a study by Huang *et al*. (2011), where short-rod MSNs were easily trapped in the liver while long-rod MSN largely distributed in the spleen after intravenous injection. The initial circulation time (2 hours) in

blood showed no difference between the particles, while measurements at 24 hours indicated a longer blood circulation time for long-rod MSNs. Additionally, short-rod MSNs were shown to have more rapid clearance from both urine and feces. Another important factor is the surface area of nanoparticles, which directly corresponds with their toxicity. Large surface area per mass makes nanoparticles more biologically active, and have the potential for inflammatory, pro-oxidant or antioxidant activity (Oberdörster, Oberdörster & Oberdörster, 2005). However, in a study by Lee, Yun and Kim (2011) MSNs with high porosity showed a reduced cytotoxic and inflammatory response compared to non-porous silica nanoparticles. The reduced toxicity was linked to less activation of mitogen-activated protein kinases, nuclear factor-κB and caspase 3.

In *in vivo* studies of mice performed by Liu *et al*. (2011), mesoporous silica particles showed a high LD50 in acute toxicity studies and no deaths were reported in repeated toxicity studies where mice were exposed to doses of 20, 40 and 80 mg/kg for 14 days. Liver abnormalities were only observed at higher doses, 500 and 1280 mg/kg for single dose studies and > 40 mg/kg for repeated dose studies. This indicates that mesoporous silica particles have low toxicity when administered intravenously and have a potential to be used for drug delivery and imaging in live animals. However, a study by Nishimori *et al*. (2009) showed that the toxicity of nanoparticles is dependent on the size of the particles. Silica particles with diameters of 70, 300 and 1000 nm were tested, and nanoparticles with a diameter of 70 nm were shown to injure the liver in single dose studies. At lower doses, the same nanoparticles caused liver fibrosis in repeated dose studies. This indicates that nanoscale materials may be hepatotoxic, but further studies are needed to examine the effect of size, shape and surface modification on toxicity.

3 *In vitro* biofilm models

The complexity and variety of microbial biofilms make them a challenge for *in vitro* testing. For controlled and reproducible testing, several “simple” biofilm model systems have been developed (Pamp, Sternberg & Tolker-Nielsen, 2009). These models can be divided into three groups; closed (static) models, open (dynamic) systems and microcosms (Lebeaux *et al*., 2013). Closed models are the simplest models and include the microtiter plate method, which is one of the most frequently used methods for biofilm testing (Stepanovic *et al*., 2007). The biofilm is grown in 96-well microtiter plates, which allows for high throughput

assay useful for studying adhesion and biofilm formation. Another closed model is the colony biofilm model, where biofilm is grown on a semipermeable membrane placed on the surface of an agar plate and transferred to fresh agar plates every 24-48 hours. The biofilm is studied using imaging methods, such as confocal microscopy, scanning electron microscopy or transmission electron microscopy (Wahlen et al., 2018). While closed models allow for easy setup and rapid testing, the limitation in nutrients and aeration as well as the buildup of waste, metabolic byproducts, dispersed and dead cells limits the usefulness of these methods (Lebeaux *et al*., 2013). In open systems, the spent culture is continuously replaced by fresh medium. However, these methods usually require specialized equipment and are less useful for high throughput analysis. The flow cell (figure 3) is an open biofilm model where a microscope slide is positioned in a flow cell subjected to the flow of medium through a peristaltic pump (Crusz *et al*., 2012). A suspension of microorganism is introduced to the flow cell and the slide is studied through microscopic observation. The system allows for control of parameters, such as nutrient composition of the medium, incubation temperature and flow rate. The drip flow reactor is another open model, where biofilms are grown on microscope slides in parallel angled test channels (Schwartz *et al*., 2010). The dip flow reactor is designed for the study of biofilms grown under low shear conditions, as the flow of medium is in a drop like manner. The third method, microcosmos, aims to more closely mimic natural ecosystems by using several bacterial species and/or material from the studied environment (Lebeaux *et al*., 2013). For example, Rudney *et al*. (2012) used hydroxyapatite and saliva to model dental biofilms. These systems try to mimic the complexity and heterogeneity of natural settings, but with more testing parameters reproducibility becomes an issue (Roeselers *et al*., 2006).

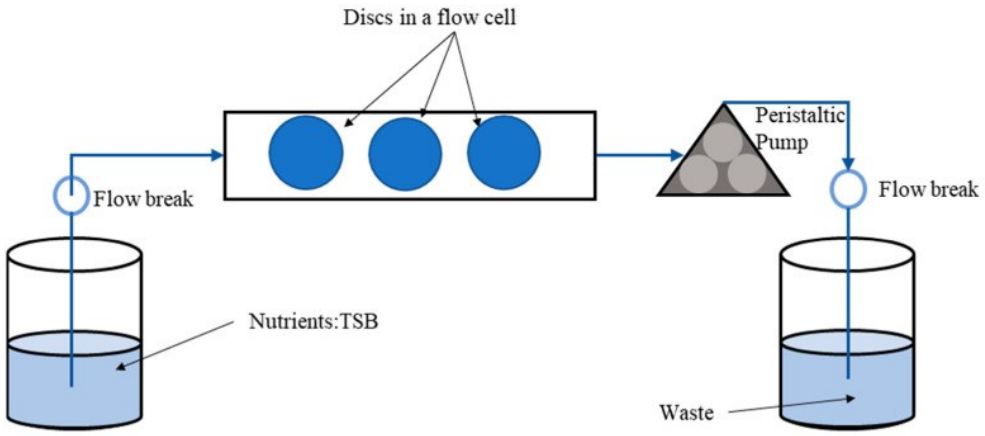

Figure 3. Schematic setup of a flow cell system (Gupta et al., 2021)

3.1 Surface plasmon resonance

Surface plasmon resonance (SPR) has become an increasingly popular technique, as it is capable of highly sensitive and specific measurements of biomolecular interactions in real time and without labeling (Taylor *et al*., 2008). SPR has been used for a wide range of applications, such as biological studies, health science research, drug discovery, clinical diagnosis, and environmental and agricultural monitoring (Singh 2016). SPR measurements can give information about specific interactions, such as binding affinity and dissociation/association rate, as well as thermodynamic parameters, such as entropy and enthalpy (Bakhitar, 2013). The SPR biosensor has a fluidic system consisting of a pump and a flow channel with the sensor. The sensor is a metal-coated glass slide with the metallic side in the flow channel and the glass side is compressed against a prism. Gold is the most commonly used metal due to its good chemical stability (Taylor *et al*., 2008). The temperature and flow rate can be controlled throughout the measurement.

SPR is based on the acceleration of surface plasmons present on the surface of a metal (Bakhtiar, 2013). When a p-polarized light beam is directed through a prism towards an interface, the light beam will under certain conditions be entirely reflected off the interface, i.e., a total internal reflection of the light beam will occur. When this occurs at the interface of two nonabsorbing media, the totally reflected light beam leaks some electrical field intensity across the interface into the other nonabsorbing media, which is referred to as the evanescent field. In SPR, the two nonabsorbing media with different refractive indices are

the metal and a dielectric medium (i.e., water or buffer). The evanescent wave excites free electrons on the metal surface within this interface, causing them to resonate. These resonating electrons, referred to as surface plasmons, are sensitive to refractive index changes on and in close vicinity of the metal surface and the surrounding environment. Changes in mass (i.e., refractive index) on the surface of the sensor are detected as a change in the resonance angle, which refers to the changes in the incident angle of the light beam that is required to excite surface plasmons when material adsorbs/desorbs on/from the sensor surface. The detection range is equal to the penetration depth of the surface plasmons into the dielectric medium (Taylor *et al*., 2008). In the interface of gold and an aqueous environment and laser wavelengths within 600–1000 nm, the detection range is between 150 and 600 nm.

3.1.1 Surface plasmon resonance for bacterial applications

SPR has been applied to a range of different biological components, such as cells, proteins, DNA, viruses, and bacteria (Chen, Ma, & Li, 2021). For bacterial detection, SPR is a promising method as it offers sensitive, specific, rapid, and label-free detection (Dudak & Boyacı, 2009). Antibodies specific to the target bacteria are immobilized on the gold sensor, and the binding of bacteria to the sensor surface is recorded. The response is proportional to the concentration of the target bacteria. SPR can be used for detection of a range of different bacteria, including *E. coli* and *S. aureus* (Maalouf *et al*., 2007; Subramanian, Irudayaraj, & Ryan, 2006). SPR has also been used to study different stages of biofilm formation. Jenkins *et al*. (2004) studied the attachment of *P. aeruginosa* on bare and modified gold surfaces. The measurement was able to distinguish between initial attachment to the sensor surface and the second, more permanent, phase of bacterial attachment. The study also compared dead and live cell adhesion, showing that the adherence is an active process that requires cell viability. Hong *et al*. (2021) used SPR to study interactions between lysins and *S. aureus* biofilm. In the study, the biofilm was cultured separately on the gold sensor and blocked with 5% bovine serum albumin (BSA) buffer before being used in the SPR measurement. Zhang *et al*. (2018) studied the effects of nanosized TiO_2 on the average thicknesses of *B. subtilis* biofilm. The study showed a decrease in biofilm thickness, increase in dispersal and reduced attachment abilities. This study suggests that SPR can be used as a method of measuring the effect of nanoparticles on biofilms.

SPR measures the change in refractive index caused by the mass accumulating on the surface of the sensor, which causes the resonance angle to shift regardless of the quality of the bond (Taylor *et al*., 2008). Therefore, bacteria attaching reversibly to the surface will also cause a change in the refractive index. When irreversible attachment occurs and bacterial cells start to divide, the surface of the sensor will be uneven and the plasmons propagation will be disturbed. This will lead to an increase in the resonance angle (i.e., the SPR peak angular position, SPR PAP) and the intensity of the reflected light (i.e., the SPR peak minimum angle, SPR PMI), showing that microcolonies have formed on the surface. A schematic representation of measuring biofilm growth within the SPR angular spectra is shown in figure 4. The SPR peak will be affected by the bacteria and EPS within the evanescent field (Zhang *et al*., 2018). For an incident light wavelength of 670 nm, this range is about 335 nm. When the biofilm mass increases, and the biofilm thickness reaches the micrometer range, then waveguide peaks will appear in the so called total internal reflection region of the SPR spectra.

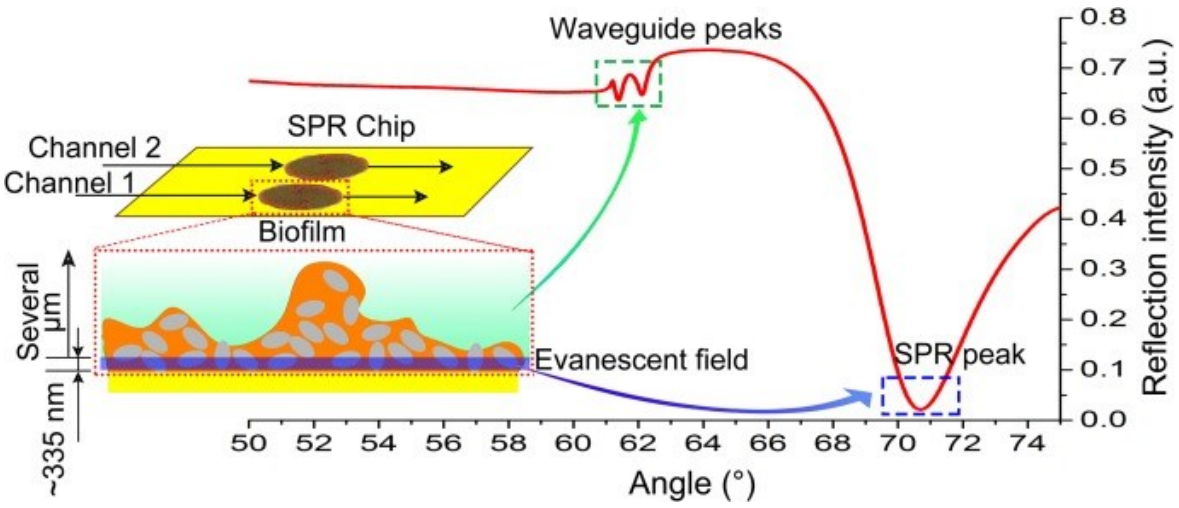

Figure 4. Schematic representation of measuring biofilm growth within the SPR angular spectra (Zhang et al., 2018).

4 Aims

The aim of this study is to examine mesoporous silica nanoparticles in the shapes of spheres and rods with different surface charges, focusing on their penetration of the extracellular matrix of *S. aureus* & *E. coli* biofilms. The study can be divided into three parts:

1. Development, optimization and functionalization of nanoparticles through several stages of characterization

2. Testing and evaluating nanoparticle penetration of *S. aureus* & *E. coli* biofilms using fluorescence microscopy, confocal microscopy and subsequent image analysis using *ImageJ* software

3. Testing nanoparticle penetration of *E. coli* biofilm using surface plasmon resonance

The main question of this study lies in the ability to evaluate labeled nanoparticle penetration with SPR, compared to the traditional ways of using fluorescence microscopy or confocal laser scanning microscopy (CLSM). SPR also offers a more comprehensive examination of biofilm formation in real time.

5 Description of research activities

5.1 Nanoparticles

The synthesis of mesoporous silica nanospheres was based on the protocol described by Desai *et al*. (2014). The origin of the reagents used for nanoparticle synthesis is listed in table 2. In short, 410.0 mg of the surfactant CTAB was dissolved in 160 ml of deionized (DI) water and gently stirred for 15 minutes at room temperature. 116.0 mg NaOH was added, and the solution was stirred for an additional 10 minutes. 40 ml EtOH was mixed in, and then 2.1 ml TEOS was added dropwise. The particles were fluorescently labeled using fluorescein isothiocyanate (FITC). For easy incorporation of FITC into the silica matrix, pre-reaction with aminopropyl triethoxysilane (APTES) was performed under vacuum for 2 hours. The fluorophore-tagged silane was added to the reaction solution right after TEOS. The solution was stirred at room temperature overnight. The synthesis solution was removed by centrifugation, after which the particles were redispersed in extraction solution (20% (m/m) NH_4NO_3 in ethanol) by sonicating the solution for 20 minutes. The extraction solution was removed by centrifugation and the extraction process was repeated once. Finally, the solution was washed once with ethanol. The prepared particles were redispersed and stored in EtOH protected from light and at a temperature of 3-8 °C.

Table 2 Origin of the reagents used for nanoparticle synthesis, labeling and functionalization.

Reagents	**Product number**	**Manufacturer**
CTAB, ≥99%	H6269	Sigma-Aldrich, USA
NaOH, for analysis	383040010	Acros Organics, France
EtOH (ETAX Aa, min. 99,5 m-%)	-	Altia Oyj, Finland
TEOS, 98%	131903	Sigma-Aldrich, USA
FITC, ≥90%	F7250	Sigma-Aldrich, USA
APTES, 99%	440140	Sigma-Aldrich, USA
$NH{\cdot}H_2O$, 32%	105426	Merck KGaA, Germany
NH_4NO_3, ≥98%	221244	Sigma-Aldrich, USA
Toluene, 99.8%	244511	Sigma-Aldrich, USA

To synthesize mesoporous silica nanorods, two different protocols were tested. In the protocol by Wang *et al*. (2013), the synthesis of differently shaped nanoparticles was based on different molar ratios of the reactants in the synthesis solution. The reactant ratios were 1 TEOS: 19.9 EtOH: x H_2O: 10.4 $NH{\cdot}H_2O$: 0.3 CTAB, were a x-value between 372 and 2,973 produced rods. In this study, x=372 and x=619 were used to synthesize rods. First, DI water, EtOH, and $NH{\cdot}H_2O$ were mixed. CTAB was then dissolved in the solution. TEOS was added dropwise. The mixture was magnetically stirred at room temperature for 2 hours. Extraction was performed twice with an extraction solvent of 2% NH_4NO_3 in EtOH and once with EtOH.

In the second protocol described by Zhao *et al.* (2017), the aspect ratio of the rods was based on different volumes of $NH_3{\cdot}H_2O$ solution. CTAB was dissolved in DI water and $NH_3{\cdot}H_2O$ (32%) was added in the volume of 2,5 ml (for short rods) or 7 ml (for long rods). TEOS was added after 30 minutes, the reaction solution was stirred at room-temperature for 5 hours and then washed with ethanol twice. The template was removed by dispersing the particles in 3% (m/m) NH_4NO_3 in ethanol and refluxed for 24 hours at 75 °C. Finally, the particles were washed once with ethanol to remove any NH_4NO_3 residues. Labeling of the rods used for testing biofilm penetration was performed in the same way as for the nanospheres.

The particles were functionalized by surface hyperbranching polymerization of polyethylenimine (PEI) according to the protocol described by Desai *et al*. (2016). 100 mg of dry particles were dispersed in 10 ml toluene. Catalytic amounts of acetic acid (5,2 µl)

and 52 µl aziridine was added and the particles were left overnight at 75 °C under reflux with stirring. The next day, the particles were washed with ethanol twice. The functionalized particles were stored in the same way as the non-functionalized particles.

Dynamic light scattering (DLS) measurements were performed to determine dispersity and approximate size of the nanoparticles. For the measurement, particles were dispersed in DI water at the concentration of 0,1 mg/ml. The surface charge of the particles was determined with zeta potential measurements. The test was performed in 10 mM HEPES buffer (pH = 7.2) at the concentration of 1 mg/ml. DLS and zeta potential were measured both before and after PEI-functionalization using a Malvern ZetaSizer instrument (NanoZS, Malvern Instruments Ltd., Malvern, UK).

Transmission electron microscopy (TEM) was used to determine the size and shape of the particles. Nanoparticles were dispersed in ethanol at the concentration of 0,1 mg/ml. A few drops of the solution were put on copper grids and allowed to dry overnight. Images were obtained using JEM-1400 Plus TEM (JEOL Ltd., Tokyo, Japan). The images were analyzed using ImageJ software to determine the diameter of the spheres and aspect ratios of the rods. A minimum of 50 individual nanoparticles were measured.

5.2 Fluorescence and confocal microscopy

A planktonic culture of bacteria was started in either tryptic soy broth (TSB, Fluka/Sigma-Aldrich, USA) for *S. Aureus* or Luria-Bertani (LB, Sigma-Aldrich, USA) for *E. coli*. The medium were prepared according to the instructions by the manufacturers and autoclaved before use. Bacteria from agar plates was added to 50 ml falcon tubes containing 10 ml medium and left overnight in 37 °C with shaking (caps loosed for aeration). The next day the cultures were diluted to a concentration of 0,01% of the planktonic over-night culture and incubated for one hour at 37 °C with shaking. 3 ml of the cultures was added to 6-well plates (for fluorescence microscopy) or glass-bottomed confocal dishes (Mat-Tek corp., USA). The plate/dishes were left at 37 °C with shaking for 18 hours. The medium and planktonic bacteria were then removed, and the biofilm was carefully washed with phosphate buffered saline (PBS, Lonza, USA) twice. 2 ml of fresh medium was added. The nanoparticles were then added to the biofilm by adding 1 ml of particles redispersed in medium at the concentration of 10 µl/ml. For control, 1 ml of plain medium was added in the same manner as the nanoparticle suspension.

For fluorescence microscopy, one well containing the sample and one control was washed and fixed after 24, 48, and 72 hours, respectively. The biofilm was washed with PBS twice and fixed with 4% formaldehyde solution (Thermo Scientific, USA) for one hour, after which the samples were washed twice with PBS again. The fixed biofilms were stored in PBS to prevent the biofilm from drying up. The images were obtained using a EVOSfl inverted microscope (Thermo Fisher, USA) with a 20x objective. For CLSM, the biofilms were incubated at 37 °C with shaking for 18 hours after addition of nanoparticles/control. The washing and fixing were performed in the same way as for fluorescence microscopy. The biofilms were imaged immediately using a confocal microscope Leica TCS SP5 (Leica Microsystems GmbH, Wetzlar, Germany) using a 100x oil immersion objective.

5.3 SPR

The gold sensor (BioNavis, Tampere, Finland) was washed prior to use in a solution of 1 part 32% hydrogen peroxide (EMD Millipore Corp, Germany), 1 part 32% ammonia solution (Merck KGaA, Germany) and 5 parts DI water. The cleaning solution was heated to the boiling point for a minimum of 5 minutes, after which the sensor was rinsed using purified water and 70% ethanol solution. After the cleaning process the sensor was placed in the SPR instrument (SPR Navi™ 200, BioNavis, Tampere Suomi) and LB medium was pumped through the flow channels for one hour by using an external peristaltic pump (MasterFlex, USA). The LB medium had been left at room temperature overnight and sonicated for 5 minutes to remove air bubbles before starting the measurement. The temperature was set at 37 °C and the flow rate at 50 µL/min throughout the measurements. After receiving the base line curve, a diluted culture of *E. coli* was injected for 30 minutes. The diluted culture of *E. coli* was prepared in the same way as for CLSM, and then incubated for one hour with shaking at 37 °C. The injection tubes were then wiped with 70% ethanol and switched back to the LB medium for 24 hours. A 500 µg/ml solution of nanoparticles in LB medium was then injected for 10 minutes, and then switched back to medium. The measurements continued for a minimum of 24 hours after injection of nanoparticles. The obtained data was analyzed using GraphPad Prism version 8.0.0 for Windows (GraphPad Software, San Diego, California USA).

6 Result

6.1 Nanoparticles

For the nanorods, two different synthesis protocols were tested. The shape and size were determined using TEM (figure 5). In the protocol by Zhao *et al.* (2017) which is based on different volumes of $NH_3 \cdot H_2O$ solution, the lower volume produced quite uniform particles with a size of 143,9 ± 38,4 nm and an aspect ratio of 2.1:1. Using a higher volume of $NH_3 \cdot H_2O$ solution produced large particles (612,0 ± 207,2 nm) with a similar aspect ratio (1.8:1). In the protocol by Wang *et al*. (2013) a change in the molar ratio of H_2O with respect to the other reagents would produce different shapes of particles. The particles produced by this protocol were both very large. The lower volume of H_2O produced rods with a size of 781.6 ± 181.3 nm, and the higher volume of H_2O rods with a size of 625.5 ± 162.7 nm. The width of the particles, however, was very different, and this consequently affected their aspect ratios. One of the particles had a width of 168.4 ±36.5 nm and an aspect ratio of 4.8:1, while the other had a width of 86.4 ± 17.3 nm and an aspect ratio of 7.3:1. The protocol by Zhao *et al*. (2017) with the lower volume of $NH_3 \cdot H_2O$ solution was chosen for preparation of nanoparticles for further testing.

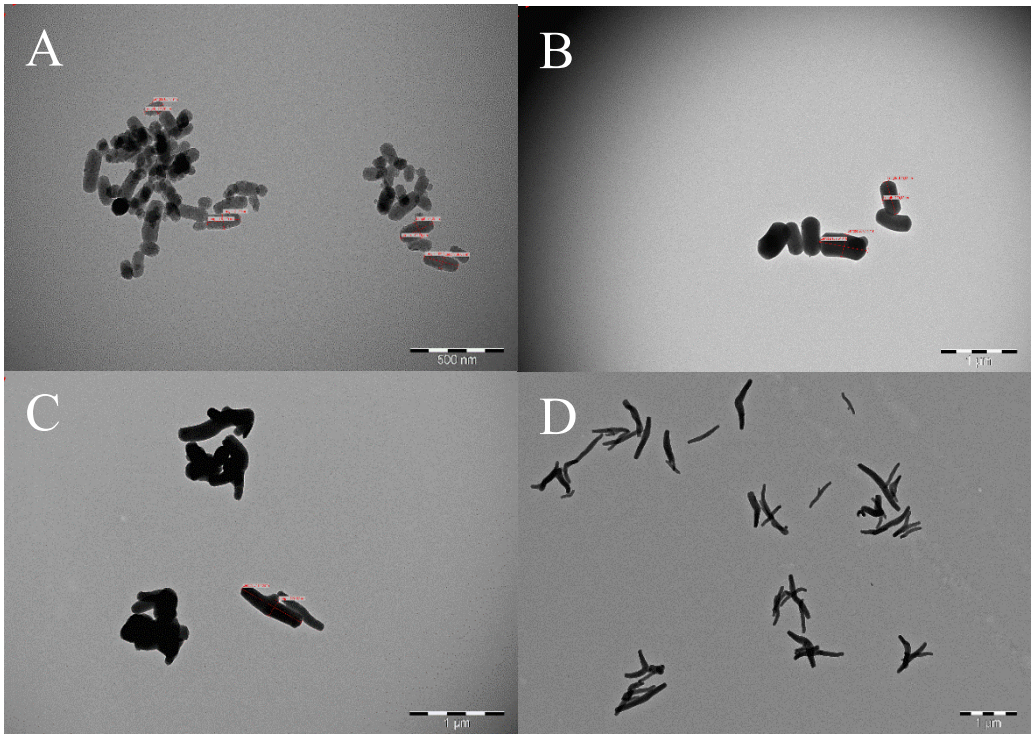

Figure 5. TEM images of the nanorods produced according to the protocols by Zhao et al. 2017 (A-B) and Wang et al., 2013 (C-D). A: short rods by a lower volume of $NH_3 \cdot H_2O$ in the synthesis solution, B: long rods

by a higher volume of $NH_3 \cdot H_2O$ in the synthesis solution, C: short rods by a lower ratio of H_2O in the synthesis solution, D: long rods by a higher ratio of H_2O in the synthesis solution. The scale bar is 500 nm for A and 1 µm for B-D.

The FITC labeled nanoparticles used for biofilm testing were characterized by DLS and ζ-potential measurements. The particle sizes measured by DLS can be seen in table 3. The spheres (MSP) showed a slightly larger hydrodynamic size of 400.7 ± 44.9 nm compared to the rods (MSR) that had a hydrodynamic size of 331.0 ± 8.7 nm. The polydispersity index (PDI) for both measurements were <0.3 showing good dispersibility and reliable size measurements. The particle sizes were measured again after PEI functionalization to provide information about the colloidal stability of the particles. The spheres (PEI-MSP) showed barely any change in particle size after functionalization, and the rods (PEI-MSR) showed a slight decrease in the particle size. PDI values were maintained under 0.3.

Table 3 Hydrodynamic particle size and PDI of the particles before and after PEI functionalization. The data is presented as a mean value of three measurements ± SD.

Sample	Particle Size (nm)	PDI
MSP	400.7 ± 44.9	0.2 ± 0.07
MSR	331.0 ± 8.7	0.2 ± 0.2
PEI-MSP	393.0 ± 14.5	0.06 ± 0.04
PEI-MSR	257.6 ± 28.7	0.13 ± 0.1

The ζ-potential was used to determine the net surface charge of the particles under given conditions, i.e. at physiological pH (HEPES buffer, pH 7.2) in the present case. Before functionalization, the particles had a negative charge (figure 6). The spheres had a ζ-potential of -14.2 ± 0.8 mV and the rods -12.3 ± 0.9 mV. The particles were surface functionalized with the cationic polymer PEI to receive positively charged particles. After functionalization, the spheres had a ζ-potential of 12.3 ± 0.8 mV and the rods 24.5 ± 1.1 mV.

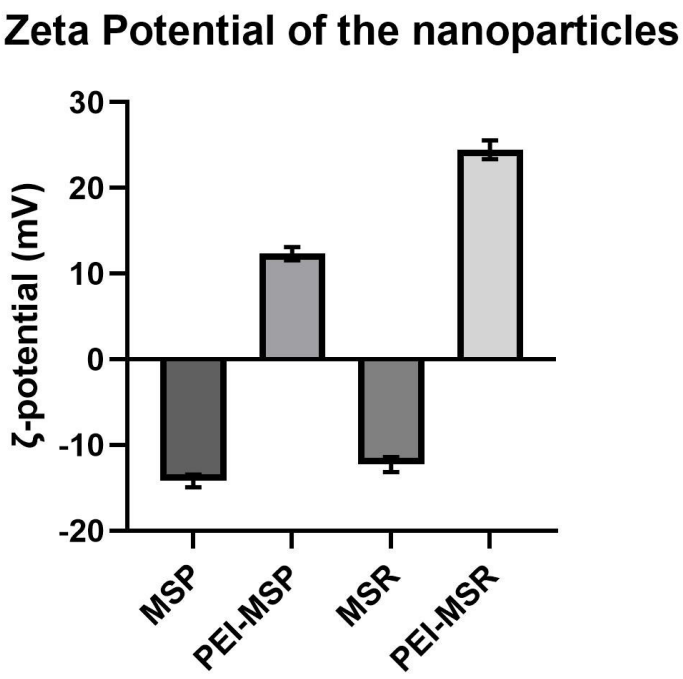

Figure 6. Zeta potential of the nanoparticles before and after PEI functionalization. The data is presented as a mean value of three measurements ± SD.

TEM microscopy was performed to provide more detailed information about the size and shape of the particles (figure 7). Imaging was performed on particles prior to functionalization. The images showed that the spheres were quite uniform in size and shape. The rods varied more in size, which might be partly because of aggregation of particles. The rods showed vertical pores with slight curvature along the length side of the particles. The analysis of the particle sizes using ImageJ showed a size of 163,1 ± 17,0 nm for MSP. For MSR, the mean length was 131,5 ± 30,7 nm and width 57,7 ± 9,4 nm. The aspect ratio for the rods was about 2.3:1.

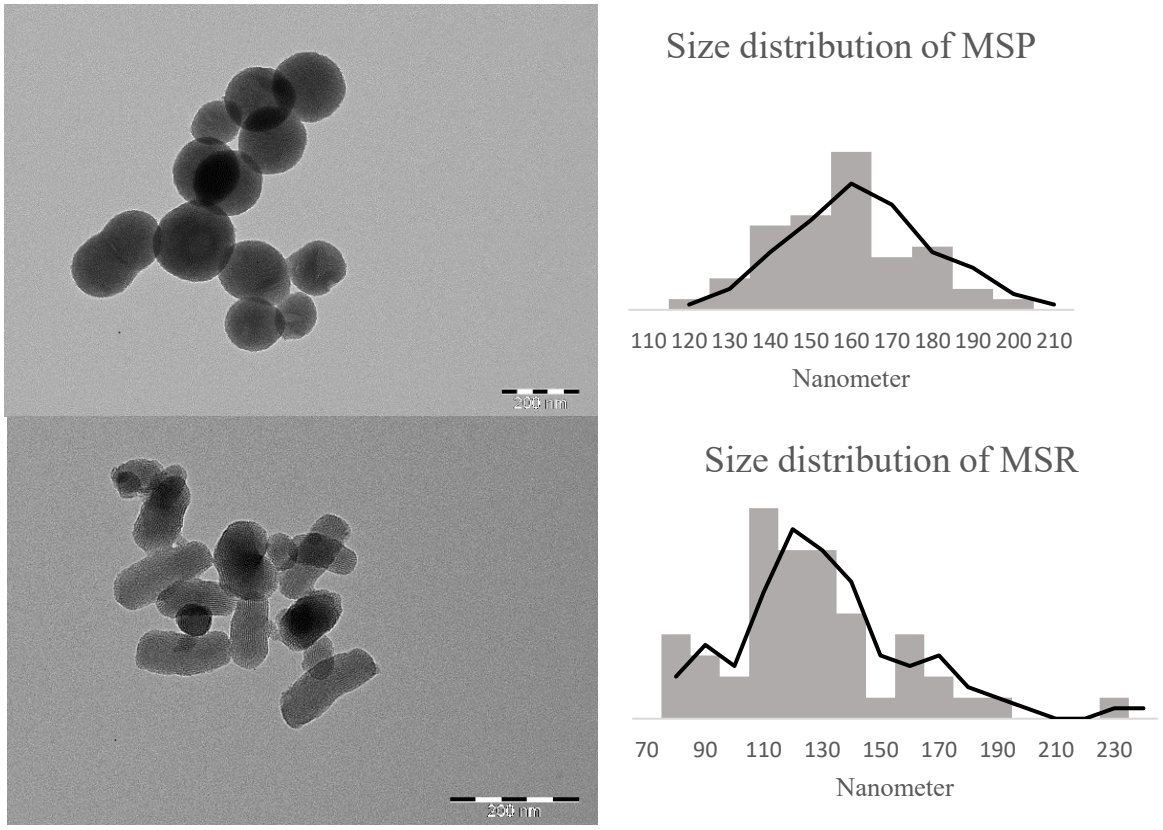

Figure 7. TEM images of MSP and MSR and the size distribution (particle diameter for spheres and length for rods) based on analysis with ImageJ software. The scale bar represents 200 nm.

6.2 Fluorescence microscopy

Fluorescence microscopy was performed to validate the biofilm testing protocol later used for confocal microscopy. Both *S. aureus* and *E. coli* were able to form a biofilm within 24 hours, however, the quality of the formed biofilms could not be determined without fluorescence staining. For *S. aureus*, the FITC labeled nanoparticles could clearly be seen in the biofilm (figure 8), suggesting that these particles were able to penetrate the extracellular matrix. There was no clear visible difference between biofilms exposed to nanoparticles for 24, 48 or 72 hours. Therefore, nanoparticles were added to the biofilm 24 hours before confocal imaging. For *E. coli*, there was no visible difference between control samples and samples containing nanoparticles (data not shown).

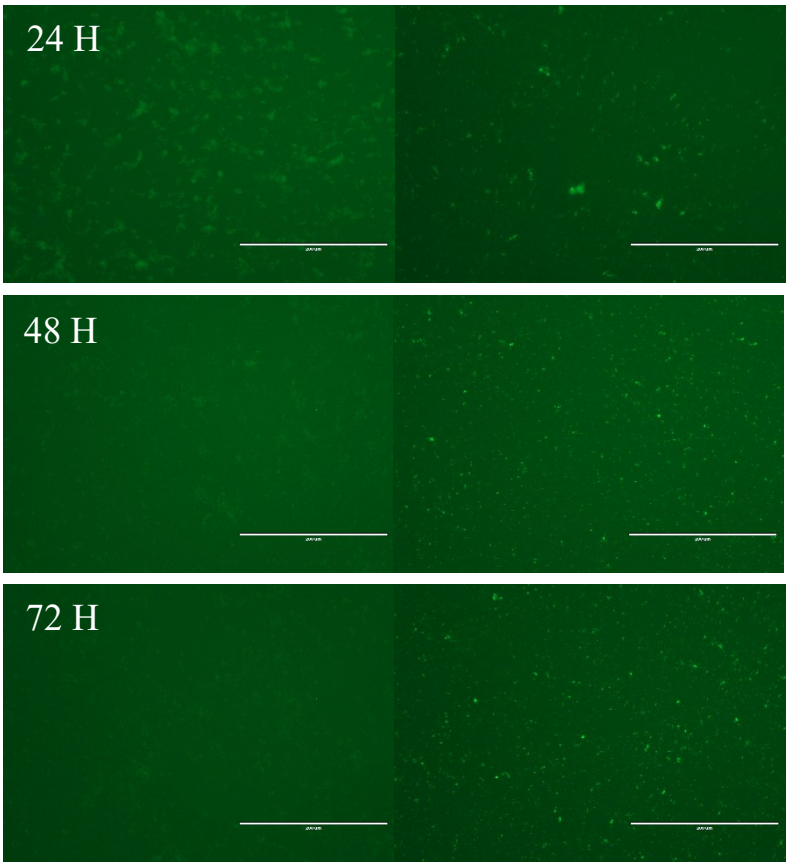

Figure 8. S. aureus biofilm imaged with fluorescence microscopy 24 h, 48 h and 72 h after addition of nanoparticles. The right column shows control, and the left column shows samples containing FITC labeled nanoparticles. The scale bar represents 200 µm.

6.3 Confocal microscopy

CSLM was performed to provide more detailed information about the location of the nanoparticles in the biofilm. Compared to fluorescence microscopy, individual bacterial cells can be visualized as well as biofilm architecture.

6.3.1 *S. Aureus* biofilm

The control sample of *S. aureus* showed a biofilm in the maturation stage where over 50% of the surface was covered with a biofilm and the biofilm was increasing in height (Figure 9A). However, the samples containing nanoparticles seemed to be in an earlier stage of biofilm formation with only microcolonies forming. Nanoparticles could be clearly seen in the samples containing MSP (figure 9B) and MSR (figure 9C). It can be assumed that the nanoparticles were able to penetrate or interact with extracellular components of *S. aureus*, as the particles would otherwise have been removed when washing the samples. However,

the particles were mainly located around the bacterial colonizes. Some of the nanoparticles were located on the surface of single cells, suggesting interactions with the cell membrane.

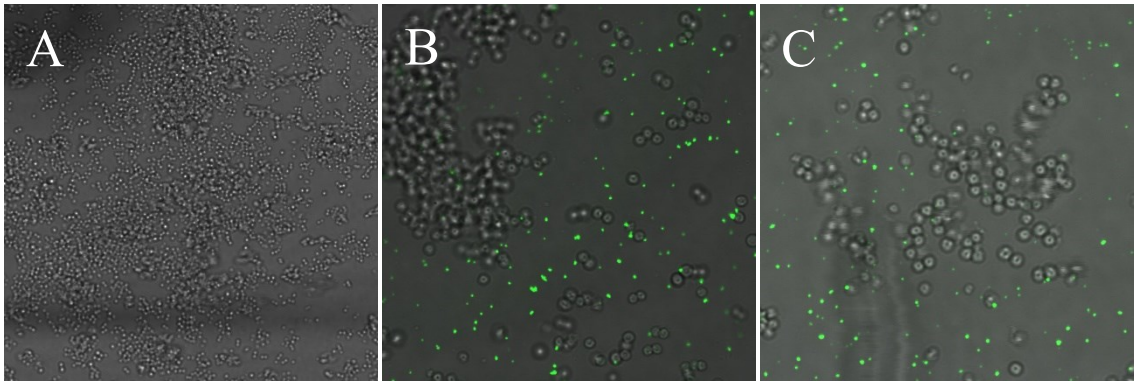

Figure 9. Confocal microscopy images of S. aureus biofilm, without nanoparticles (A), with MSP (B) and with MSR (C).

With regards to PEI-functionalized particles, no particles could be found in the sample containing PEI-MSP (figure 10A). If the particles were unable to penetrate the biofilm, they would have been removed during the washing process. Interestingly, the biofilm in this sample more closely resembled the biofilm in the control sample, as it covered more area of the surface and was growing vertically as well. For PEI-MSR, the result was similar to MSP and MSR. The areas containing the most nanoparticles were also the areas with the lowest bacterial cell concentration.

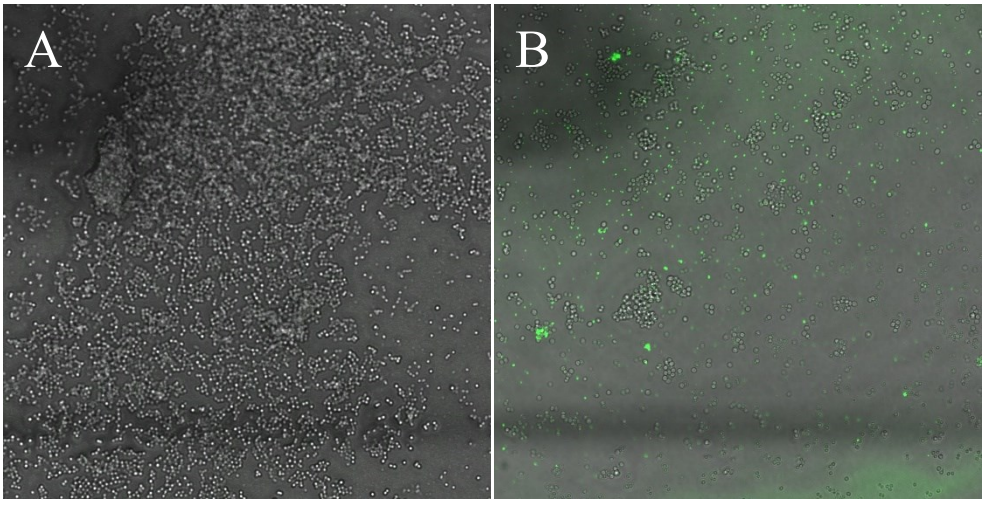

Figure 10. Confocal microscopy images of S. aureus biofilm, with PEI-MSP (A) and with PEI-MSR (B).

6.3.2 *E. Coli* biofilms

For *E. coli*, the biofilm formation was more uniform between the control sample and samples containing nanoparticles. After 48 hours microcolonies of different sizes had formed and the biofilm had started to become thicker. However, there was a lot of variation between different areas of the confocal dish. The nanoparticles seemed to be less able to interact with *E. Coli* biofilms compared to *S. aureus* biofilms. In the samples containing MSP and MSR, nanoparticles could be seen (figure 11A-B), but in a significantly smaller amount compared to the *S. aureus* samples. There was no indication that the nanoparticles were able to penetrate deeper into the biofilm and they seemed to be in the outer layer of the extracellular matrix. However, this could be hard to determine as many of the samples only contained a monolayer of bacteria. Most of the nanoparticles detected was concentrated to the colonizes of *E. Coli* bacteria, while for *S. aureus* samples the nanoparticles were in areas not containing any bacteria. This could suggest that the nanoparticles interacted with the *E. coli* bacteria themselves rather than the extracellular matrix. As for the PEI-functionalized particles, neither PEI-MSP nor PEI-MSR could be detected in the samples (figure 11C-D).

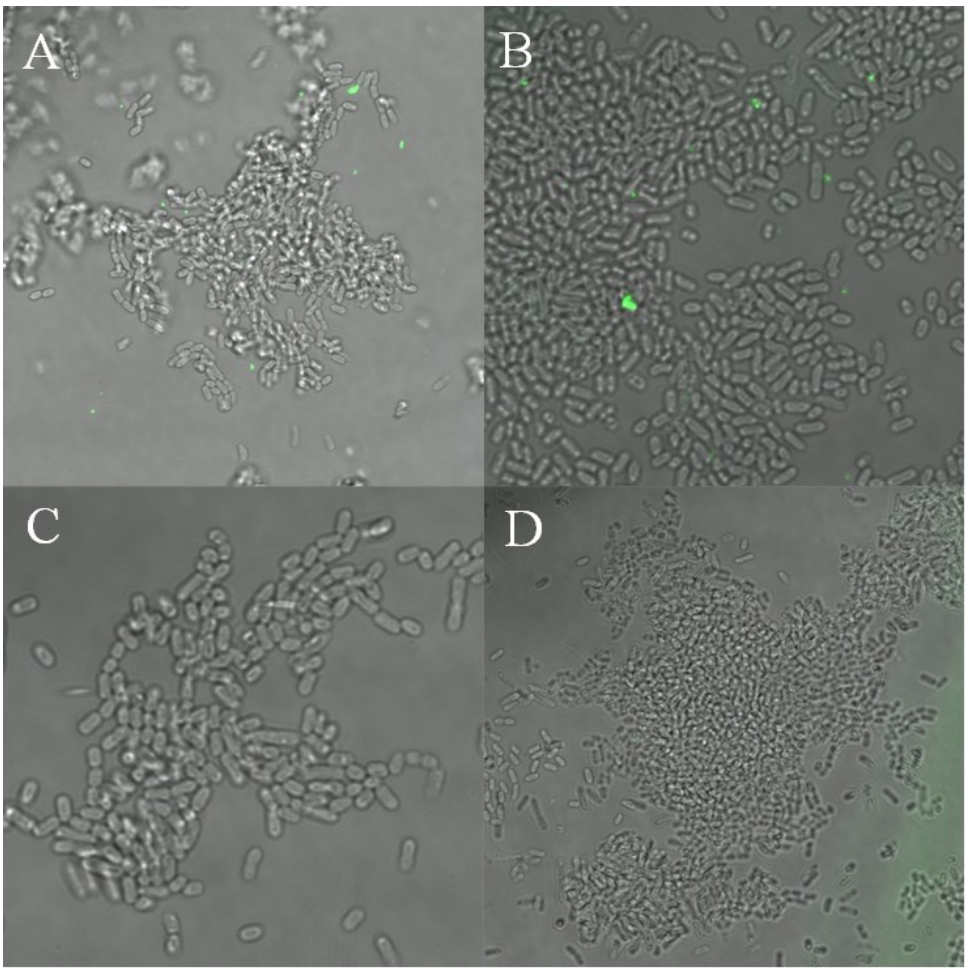

Figure 11. Confocal microscopy images of E. coli biofilm, with MSP (A), MSR (B), PEI-MSP (C) and PEI-MSR (D).

6.4 SPR

6.4.1 *E. coli* biofilm growth

The biofilm growth of *E. coli* monitored with SPR in real time was quite uniform for all measurements (figure 12). A very slow increase in the SPR PAP could be seen for about two hours after injecting the bacteria solution into the SPR flow channels. After this a rapid increase in the SPR PAP could be seen. This suggests that only a small fraction of bacterial cells initially adheres to the gold sensor, and that an irreversible attachment of these bacteria takes place during the first two hours after injection into the SPR flow channels. The large increase in the SPR PAP after approximately two hours suggests a rapid increase of the mass on the sensor surface, which indicates that the biofilm enters the maturation stage and that cells divides rapidly during this phase. The increase in the SPR PAP levelled out after about 6-7 hours after bacteria injection into the SPR flow channels. This suggests that the biofilm

stopped growing at this point and reached its final thickness under these experimental conditions (i.e., 37°C and 50 µl/min flow speed).

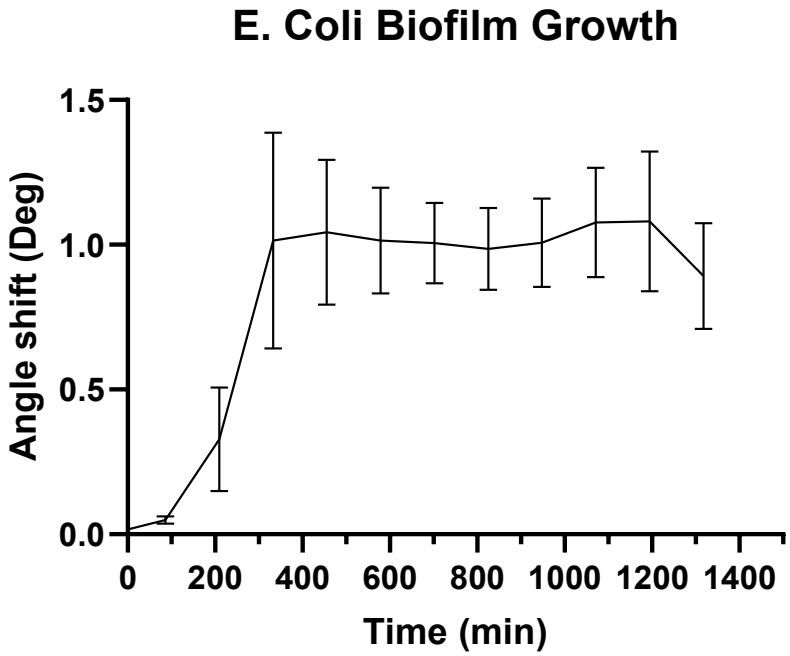

Figure 12. E. coli biofilm growth measured with SPR. The data shows the mean and SD of the change in the SPR PAP from six measurements.

The shift in the SPR PMI was simultaneously measured with the shift in the SPR PAP during *E. coli* biofilm growth. Figure 13A shows the change in the SPR PAP and PMI for one *E. coli* growth measurement. The SPR PMI started to increase earlier than the SPR PAP after injection of the bacteria into the SPR flow channels and reached its peak value after about 100-200 minutes, after which the SPR PMI declined and levelled out after about 200-300 minutes. The increase in SPR PMI is probably due to scattering of the light from small colonies of bacteria that form and grow on the sensor surface with time. This is supported by the fact that the SPR PMI is decreasing and returns almost to its initial value when the biofilm has formed, i.e., the biofilm has become a smooth homogeneous layer which is when the SPR PAP reached its maximum value. Changes in the total internal reflection (TIR) region of the full SPR angular spectra could also be seen during the growth of the biofilm. At 400 minutes the TIR region had become smoother compared to the point before any significant biofilm had formed (i.e., 40 min), and after 20 hours (1200 min) additional waveguide peaks had formed in the TIR region, which suggests that a thick biofilm had been formed on the sensor surface.

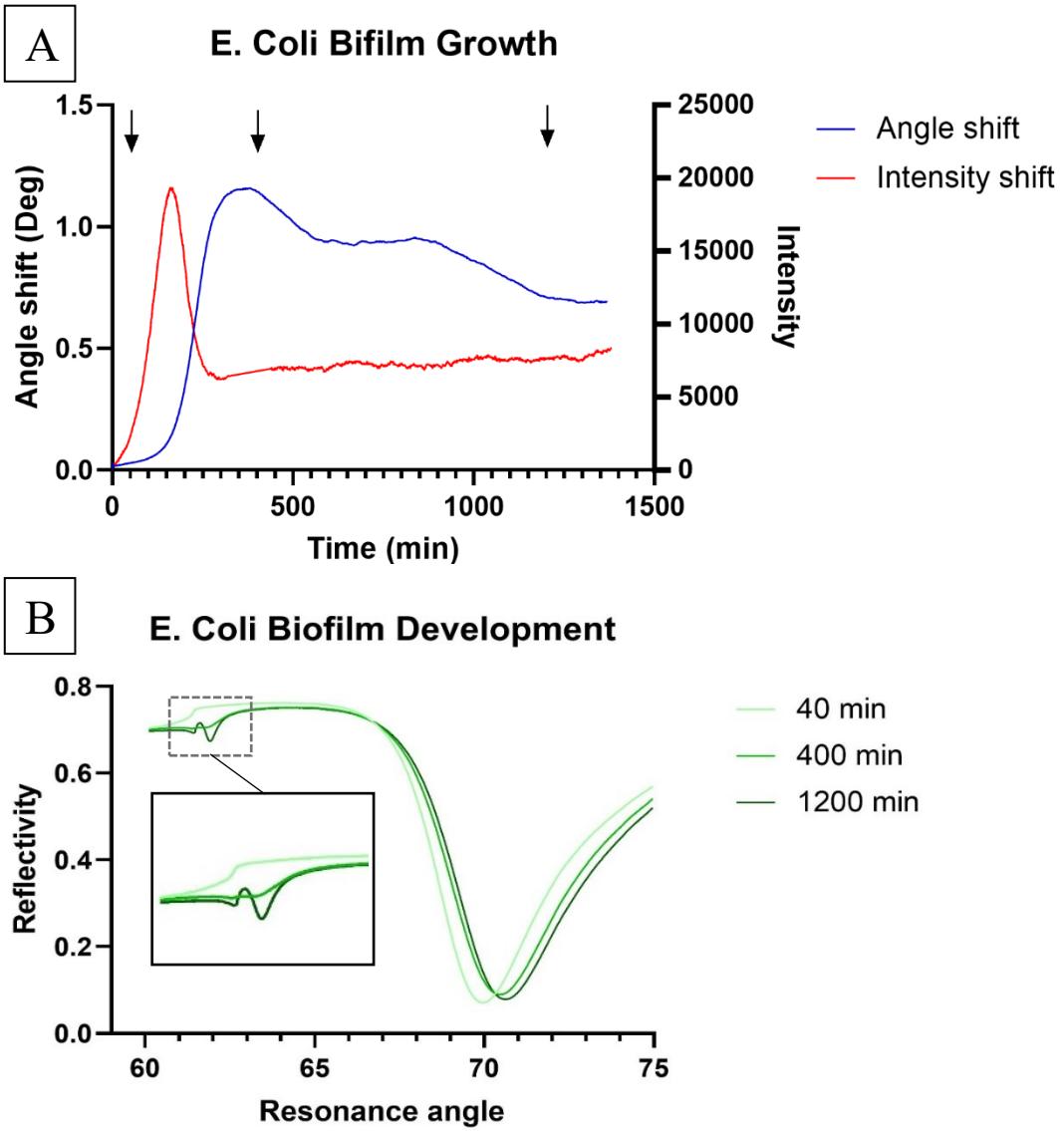

Figure 13. E. coli biofilm growth measured with SPR. A: the changes in the SPR PMI and the SPR PAP for one measurement. B: the full SPR angular spectra at the timepoints marked with the arrows in the first graph.

6.4.2 Effect of nanoparticles on *E. coli* biofilms

The SPR measurement continued for a minimum of 24 hours after the addition of nanoparticles. For MSP, no changes in the SPR PAP or SPR PMI could be seen during this time (figure 14A). For PEI-MSP, on the other hand, a slight increase in both the SPR PAP and SPR PMI could be seen (figure 14B). Accumulation of nanoparticles in the biofilm would show a constantly growing signal that would level out when the particles reach the

evanescent field region. This plateau was not reached during the 24 hours this measurement continued.

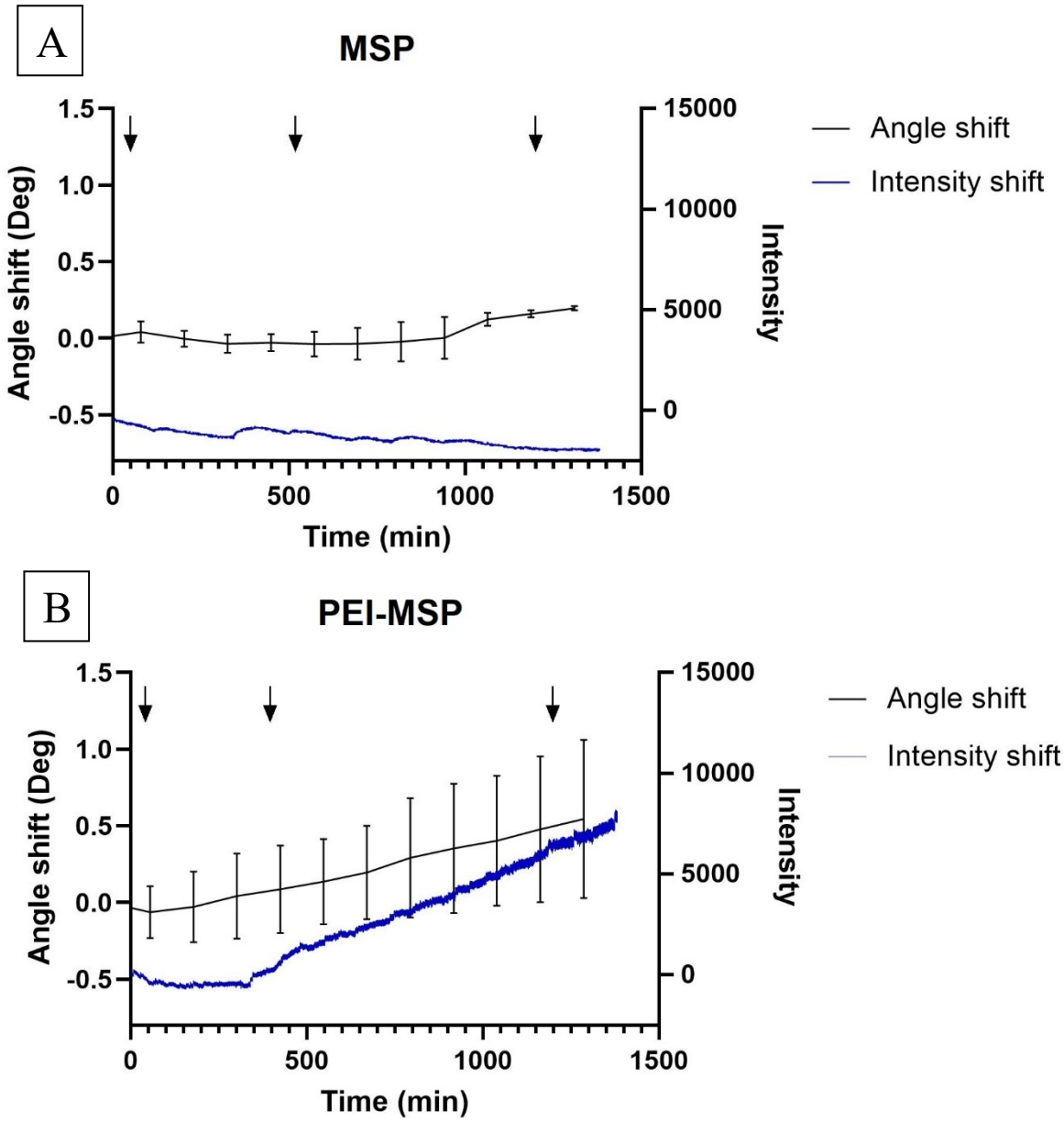

Figure 13. Angle shift and change in the intensity of the reflected light after addition of MSP (A) and PEI-MSP (B). Both angle shift results are the mean of three measurements with SD. The intensity shift is presented as an example from one of the measurements. The arrows show the timepoints for the SPR angular spectras shown in figure 15.

As the shift in SPR PAP only represents the changes in the evanescent field, it does not represent the biofilm as a whole. Therefore, the full SPR angular spectra was studied to determine the nanoparticles effect on the biofilm in the micrometer scale. For the

measurements included, at least one waveguide peak was visible in the TIR region of the full SPR angular spectra before the injection of nanoparticles, which suggests the presence of a thick biofilm on the sensor surface. After the injection of nanoparticles, the TIR region of the full SPR angular spectra would smoothen out and the waveguide peaks would disappear (figure 15). This was visible in both measurements of MSP and PEI-MSP. After 40-50 minutes, the waveguide peaks would still be there, but after 6-8 hours the change was already apparent. No major change happened between hour 6-8 and the end of the measurement at 20 hours (1200 min). This suggests some kind of change in the biofilm structure and thickness after injection of nanoparticles even if it was not visible or apparent in the shifts of SPR PAP and SPR PMI.

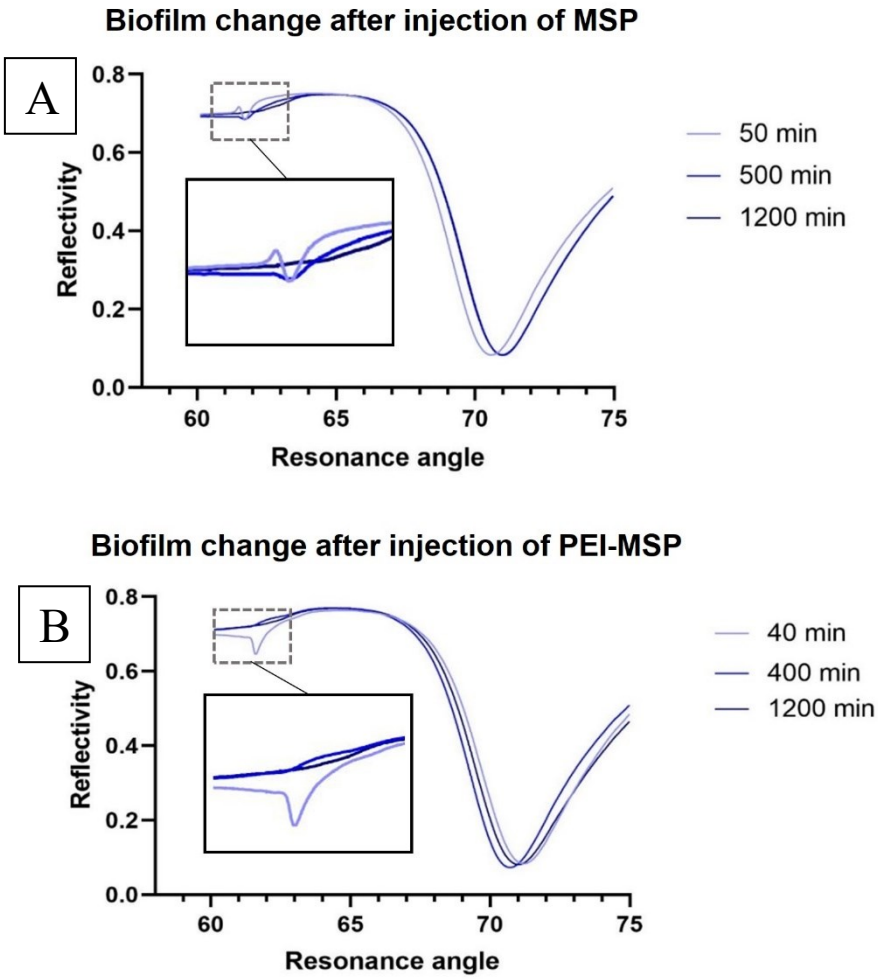

Figure 14. Change in the full SPR angular spectra after injection of MSP (A) and PEI-MSP (B). The data is for one measurement representing the three measurements conducted for both nanoparticles.

7 Discussion

7.1 Nanoparticles

The mesoporous silica particles produced for this study showed good qualities for their intended use. The DLS measurement showed full redispersibility of particles in water, and a low PDI value indicating a narrow particle size distribution. DLS measures the hydrodynamic size, which is influenced by the hydration layer forming around the particles in solution. Particle size measured with DLS are, therefore, usually considerably larger than the sizes measured by other techniques (Kaasalainen *et al*., 2017). The TEM imaging revealed uniformed particles in a size range below 250 nm. The shape and size of particles affect the drug-loading efficiency (Chen *et al*., 2012). However, the size will also determine the biofilm penetration ability of the particles, and a smaller size is usually considered favorable (Peulen & Wilkinson, 2011). In a study by Li *et al*. (2016), mesoporous particles of a similar size as the one in this study (i.e., spheres with an average diameter of 265 nm and wires with a width of 53 nm and length of 477 nm) were able to penetrate biofilms of an oral origin. Additionally, both particles showed promising drug-loading capabilities. For further testing of the particles in this study, qualities important for drug delivery applications, such as drug-loading, release profile and toxicity, would have to be evaluated.

7.2 Biofilm formation

The first and critical stage of biofilm formation is the attachment of bacteria to a surface. The adhesion process varies depending on the specific bacteria (An & Friedman, 1998). *S. aureus* uses a range of different surface proteins to attach to surfaces, such as BAP (Cucarella *et al*., 2001). For *E. coli*, curli protein is important for attachment as increased curli production is generally connected to higher adhesion to glass surfaces (Goulter, Gentle & Dykes, 2010). For both *E. coli* and *S. aureus*, initial attachment to glass surfaces have been shown to happen within the first hour of introducing planktonic bacteria to the surface (Li *et al*., 2017). In this study, *S. aureus* and *E. coli* were able to attach to the glass surface of the confocal dishes within 24 hours.

The SPR measurement showed that only a small number of bacteria initially attaches to the gold sensor surface, which was seen as a slow increase in the SPR PAP which indicates

irreversible attachment of bacteria to the sensor surface. The rapid increase in the SPR PMI during the first two hours after injecting the bacteria indicates the formation of microcolonies of bacteria on the sensor surface, which scatters the reflected light. The SPR PMI reaches its peak when the growth of the extracellular matrix is increasing and forming a homogenous layer embedding the bacteria islands, which causes the SPR PMI to decline as there is no more scattering of light. While both SPR PMI and SPR PAP are affected by an increase in number of bacteria on the surface, the SPR PAP continues to increase as the SPR PMI levels out, as it reflects both the mass of bacteria and of the extracellular matrix.

The formation and structure of a mature biofilm is influenced by several factors, such as nutrient availability and flow (Teodósio *et al*., 2011). Fallarero *et al*. 2013 showed that *S. aureus* will be in an active growth stage for up to five hours after attachment, after which the biofilm will reach a plateau phase. For *E. coli* biofilms the process of biofilm formation is slower. Lüdecke *et al*. (2014) studied *E. coli* biofilm adhesion and formation on different surfaces in a flow-cell system. The adhesion was studied as two different phases, initial lag-phase I with no or slow bacterial adhesion and a phase of fastest adhesion II. On a glass surface, the lag-phase I lasted for 16 h followed by the fast adhesion phase with an increase of coverage of 0.09% per hour. In this study, similar results were seen when comparing the different species of bacteria. In the control samples, *S. aureus* covered a significantly larger portion of the surface than *E. coli*. In the SPR measurements, *E. coli* biofilms were formed after 6-7 hours. The production of extracellular substances could be seen after about 2-3 hours, when the SPR PMI decreased. Additional peaks, i.e., waveguide peaks, in the TIR region of the full SPR angular spectra suggests that a thick biofilm in the micrometer scale was formed after about 20 hours.

Dispersion is the final stage of biofilm formation, where cells escape the extracellular matrix to migrate to new locations. Although thinning of the biofilm would be observable in SPR measurements, dispersion rarely happens at the same time for the entire biofilm (Purevdorj-Gage, Costerton & Stoodley, 2005). Usually, only specific areas or microcolonies will disperse at the same time. The timing for dispersion varies greatly in different studies, with time frames ranging from 15 minutes to 40 hours in biofilms allowed to grow in a range of 2 hours to 10 days (Petrova & Sauer, 2016). When dispersion occurs, there will be microscopically observable hollow mounds in the biofilm (Purevdorj-Gage, Costerton & Stoodley, 2005). Theoretically, this change in surface morphology could cause a change in the SPR PMI, but for thicker biofilms the change would probably not be as noticeable. In

this study, changes in the TIR region of the full SPR angular spectra suggests structural change to the biofilm after nanoparticle injection. This could indicate sloughing or removal of bacteria from the biofilm, which could leave a thinner biofilm or a collapsed extracellular matrix film on the surface of the sensor. However, here is no way to distinguish between the active form of dispersion and the inactive form of erosion or sloughing which probably will occur in a system with an active flow.

7.2.1 SPR compared to CLSM as a biofilm model

In this study, *E. coli* biofilm was grown on two distinctly different surfaces, glass for CLSM studies and gold for SPR studies. As the growing conditions were distinctively different, no straight comparisons between these techniques and surfaces can be made. However, it should be noted that a biofilm was formed on both surfaces. The properties of the surface will affect not only the attachment but also the formation of the biofilm. Both *E. coli* and *S. aureus* have shown greater attachment and higher production of extracellular substances when grown on a rough surface compared to a smooth surface (Mitik-Dineva *et al*., 2008). As far as clinical biofilms are concerned, the hosting surface can be anything from a medical device, such as a urinary tract catheter or prosthetic joint, to tissues in cystic fibrosis or wound infections (Lebeaux *et al*., 2013). This is a challenge of *in vitro* biofilm models, as biofilms may act completely differently when growing on different host surfaces. It has been shown that bacteria will behave differently when attached to different surfaces, such as glass, metal or plastic (Fletcher & Loeb, 1979).

The two different biofilm models used in this study can be classified as a closed (static) system and an open (dynamic) system, respectively. In the CLSM study, biofilms were grown in a closed system where the medium was replaced after 18 hours. In the SPR measurements, there was a continuous flow of medium. For *E. coli*, nutrient availability has been shown to affect both the switch from planktonic to biofilm growth, as well as biofilm architecture (Teodósio *et al*., 2011). However, the continuous flow of medium will also increase the shear stress on the biofilm. A high shear stress will lead to the detachment of cells from the surface (Zhang *et al*., 2011). In slow flow conditions, biofilm formation can be uneven, as areas with high fluid influx will receive higher inputs of oxygen, carbon, and nutrients. When nutrient flow is limited, biofilm will adopt a less dense architecture with water channels to evenly distribute the nutrients throughout the biofilm (Teodósio *et al*., 2011). This form of biofilm is not very resistant to shear stress. Under turbulent conditions,

a denser biofilm structure is preferrable. Although the biofilm was not optically observed during the SPR measurement, the change in the SPR PAP suggested that a thick biofilm in the micrometer scale was formed. In the confocal dishes, only a thin monolayered biofilm had formed after 48 hours. The difference in biofilm formation may well be due to differences in nutrient flow and shear stress. As a biofilm model, a dynamic system will more closely represent clinical infections, where bacteria must withstand the flow and shear stress in blood vessels (Grubb *et al*., 2009).

In SPR, the evanescent field only stretches some hundred nanometers into the biofilm, while the biofilm can grow several micrometers thick (Zhang *et al*., 2018). SPR provides detailed information about biofilm attachment and early formation, but for later stages in biofilm maturation the information is limited to biofilm thickness. For thick biofilms, CLSM holds an advantage as it can image the biofilms in different sections of the z-axis, providing important information about biofilm structure (Pamp, Sternberg & Tolker-Nielsen, 2009). CLSM also allows for fluorescence staining of the bacteria, giving further information about bacteria viability and accumulated biomass. It is also possible to stain specific components of the extracellular matrix, providing valuable information about the composition of the biofilm (Lawrence, Neu & Swerhone, 1998).

7.3 Nanoparticles effect on biofilm

The accumulation of nanoparticles in biofilms has been widely studied for its environmental implications. For example, a study by Ferry *et al*. (2009) showed that the majority of gold nanoparticles introduced to a marine mesocosm accumulated with biofilms rather than other parts of the system (sediments, seagrass, bivalves, shrimp and plankton). While the accumulation of wastewater nanoparticles in natural biofilms may have severe negative effect on the microbial life, this effect is desired when developing nanoantibiotics.

7.3.1 Penetration of biofilm

The penetration ability of nanoantibiotics in biofilms is crucial for its efficacy. The penetration can be divided into three steps: transport of nanoparticles to the biofilm–fluid interface, attachment to the biofilm surface and migration within the biofilm (Ikuma, Decho & Lau, 2015). This process is regulated by biofilm properties, such as viscosity and cell density, surrounding conditions (for example liquid flow) and the properties of the

nanoparticles. Size is one of the most important factors, as Peulen and Wilkinson (2011) found that the self-diffusion coefficient decreases with increasing nanoparticle size. It was also found that size was a particularly regulating factor in dense biofilms, where nanoparticle self-diffusion became severely limited when the size was larger than 50 nm. In this study, nanoparticles with a size of <500 nm were able to penetrate biofilms. There was also no significant change in penetration based on the shape of the particles. Slomberg *et al*. (2013) tested different sized and shaped nitric oxide-releasing silica nanoparticles against Gram-negative *P. aeruginosa* and Gram-positive *S. aureus* biofilms. Smaller sizes and higher aspect ratios were more effective against both *P. aeruginosa* and *S. aureus* biofilms. Rod-like particles were more effective than spherical particles in delivering NO and inducing degradation of the biofilm. As rod-shaped nanoparticles have showed higher drug-loading capability due to higher surface area (Chen *et al*., 2012), they show a high potential for transporting antibiotics into biofilms. Surface charge is another factor regulating biofilm penetration. Li *et al*. (2015) studied the *E. coli* biofilm penetration ability of quantum dots with different surface properties. It was found that neutral and anionic particles were unable to penetrate the biofilm. Cationic particles, however, were able to penetrate fully into biofilms. With CLSM, the opposite was noted in this study. While penetration was low for negatively charged particles, the positively charged nanoparticles did not seem to interact with *E. coli* at all. It should, however, be noted that the study by Li *et al*. (2015) used three-day-old biofilm to examine penetration, which would give a much thicker biofilm. Also, as the negatively charged particles were located around the bacteria in this study, it is possible that the interactions were with the bacteria themselves rather than the extracellular matrix. To accurately determine the penetration of nanoparticles into biofilms, thicker biofilms would be preferred. At least for *E. coli*, a protocol with a longer incubation time would be recommended. For SPR, PEI-MSP seemed to be able to penetrate the biofilm as a slight increase in both the SPR PAP and SPR PMI suggests accumulation of nanoparticles in the biofilm. For the particles to reach the evanescent field and the signal leveling out, an additional measuring time of 24-48 hours would be recommended.

7.3.2 Biomolecular corona

When nanoparticles come into contact with biofilm, they will interact with a variety of biological macromolecules that will inevitably change the surface properties of the particles, which is called a biomolecular corona (Fulaz *et al*., 2019). While proteins are the most

studied corona component, other biomolecules are also involved (Monopoli *et al*., 2012). Biomolecular corona further complicates the predictions of biofilm and nanoparticle interactions, as its mechanism of formation is not yet fully understood. The composition and evolution of the biomolecular corona are affected by several different factors, such as exposure time, temperature and nanoparticle size, surface charge and hydrophobicity (Docter *et al*., 2015). It has been suggested that negatively charged nanoparticles will interact primarily with positively charged proteins and vice versa. The interactions with cell membranes and the cellular uptake of nanoparticles are believed to be partially controlled by the adsorbed proteins. Understanding the mechanism of biomolecular corona formation is, therefore, critical for understanding the biofilm penetration of nanoparticles. SPR has been suggested as a method for this, as interactions between nanoparticles and specific biomolecules could be detected (Canovi *et al*., 2012).

7.3.3 Microbial toxicity of nanoparticles

While MSNs are generally considered safe, there are very little studies regarding the microbial toxicity of MSNs. In a study by Son and Lee (2021), the toxicity of MSNs against *E. coli* was studied. They showed that the toxicity of MSNs against microorganisms was dependent on the residual CTAB in the MSNs. CTAB is cytotoxic and can disrupt cell membranes (He *et al.,* 2010). Size is also a critical factor, as smaller nanoparticles tend to show higher cytotoxicity. Mathelié-Guinlet *et al*. (2017) showed that silica nanoparticles had a cytotoxic effect on *E. coli* bacteria in the size range of 50–80 nm. The damage was explained by membrane penetration of small nanoparticles. Larger nanoparticles showed similar damage when positively charged. Positively charged silica particles with a size of 100 nm showed similar damage as negatively charged particles of the smallest size.

In this study, biofilm formation by *S. aureus* was notably inhibited in the presence of nanoparticles, while *E. coli* was less affected. One explanation of this is interactions with the bacterial cell itself. Cell-nanoparticle interactions are affected by the cell wall charge of the bacteria (Hajipour *et al*., 2012). *S. aureus* is a Gram-positive bacterium with a cell wall containing a thick layer of peptidoglycan attached to teichoic acids (Scott & Barnett, 2006). *E. coli* is a Gram-negative bacterium which, in addition to a peptidoglycan layer, has an outer membrane composed of a phospholipid bilayer, containing lipopolysaccharides and proteins (Mathelié-Guinlet *et al*., 2017). The outer membrane makes gram-negative bacteria less sensitive to hydrophobic compounds. If the nanoparticles induced cytotoxic effects on

the bacteria, the dead bacteria would be removed in the washing process, as attachment has been shown to be an active process requiring cell viability (Jenkins *et al*., 2004). This could explain the large number of nanoparticles in areas not covered by *S. aureus* biofilm. It is also possible that the nanoparticles interacted with the extracellular matrix, causing structural failure or dispersion. The complexity of the extracellular matrix and its components makes the need for targeted studies inevitable to understand the anti-biofilm effect of nanoparticles.

7.4 SPR as a biofilm testing model

The extracellular matrix has been called the "dark matter" of biofilms (Flemming, Neu & Wingender, 2017). The extracellular matrix makes biofilms a complex, dynamic and diverse form of growth. There is a great variety in biofilm growth and composition not only between bacterial species but also within the same species, depending on conditions, such as host surface, nutrient availability, and flow. This makes biofilm models in laboratory settings a challenge. Biofilm model systems need to be controllable, constant, and reproducible (Lüdecke *et al*., 2014). SPR measurements are highly sensitive and offer the possibility to measure biofilm formation in real time. However, there are some limitations of the method. For one, measurements are time-consuming, as the number of measurements is limited to the number of flow channels. SPR can also be classified as a "once-through" system, where the fluid is discarded after passing through the flow cells, which requires the constant preparation of culture medium which can be time-consuming and cost-ineffective (Teodósio *et al*., 2011).

There are very limited studies on the use of SPR to study biofilms. However, as a set-up, the system can be compared to the flow cell system. One problem that can arise when using SPR is air bubbles in the system. Air bubbles not only affect the stability of the flow of medium, but they can also remove cells from substratum while passing through (Pamp, Sternberg & Tolker-Nielsen, 2009). In the flow cell system, bubble traps are widely used to prevent air bubbles from reaching the flow cell. In a bubble trap, the medium passes from an inlet through a syringe cylinder and out through an outlet positioned lower than the inlet. Any passing air bubbles will float to the top of the cylinder and are prevented from passing through the outlet. In this study, the use of an external pump significantly reduced the number of air bubbles in the system. The medium was also sonicated prior to use in order to

remove air bubbles. Contamination is another issue when working with bacteria. In order to maintain as consistent a system as possible, the tubes were wiped off with 70% EtOH after the injection of bacteria. However, it became clear after each measurement that the medium was contaminated and there was planktonic bacterial growth. This could be observed optically, as the medium would go from clear to cloudy after 48 hours. This means that there was constant introduction of planktonic bacteria to the system. If the SPR measurement aims to study the eradication of biofilms, the addition of planktonic bacteria could lead to reformation of the biofilm. For a stable and consistent system, the asepsis of the system would need to be addressed.

While SPR measures the accumulated mass on the sensor surface, it gives no information about the quality of the biofilm, for example the cell density or the ratio of dead and alive cells. As a model for antibacterial components, it may not be suitable as the killing of bacteria may still leave behind other components of the biofilm (Koo *et al*., 2017). As a testing method, it is more suitable for anti-biofilm agents that aims to reduce adherence, disrupt formation or eradicate biofilms. Several models combining SPR imaging with additional imaging modalities, such as bright-field, epifluorescence, total internal reflection microscopy and SPR fluorescence microscopy have been developed (Su, Fang & Li, 2021). For example, Abadian *et al.* (2014) used Surface Plasmon Resonance imaging (SPRi) to visualize *E. coli* and *P. aeruginosa* biofilm formation and removal. SPR, therefore, holds a high potential for development in biomedical applications.

The limitation of any *in vitro* model is its ability to accurately represent an *in vivo* model or clinical studies (Lebeaux *et al*., 2013). Biofilms formed in the body usually have a more complex structure due to interactions with host biomolecules and blood cells (Yasuda, Koga & Fukuoka, 1999). A biofilm formed on a gold surface may also differ vastly from a biofilm formed on tissue. By immobilizing living cells or extracellular membranes by denaturant on the sensor chip, the system would more closely represent *in vivo* models (Su, Fang & Li, 2021). By this method, the formation of biofilms on different surfaces could also be studied. It could also be a possibility to study multispecies biofilm by SPR measurements. Nearly all natural biofilms contain more than one species of bacteria (Elias & Banin, 2012), so the use of multispecies biofilm models will more closely represent biofilms in clinical settings. However, the use of more complex models comes with its own challenges in terms of reproducibility and stability, and the model should be applied accordingly to what information is being sought after.

In a clinical setting, it takes several days for a bacterial biofilm to form and several days longer to see the therapeutic effect of a drug (Yasuda, Koga & Fukuoka, 1999). An *in vitro* system should, therefore, be able to continue under stable conditions for a longer time. It has also been shown that the antibiotic resistance of biofilm increases with biofilm age (Singla, Harjai & Chhibber, 2013). In this study, the biofilms tested were grown for 24 hours before adding nanoparticles. If measuring biofilm development over a longer period of time with SPR, certain problems should have to be addressed, such as the contamination of the medium and potential biofilm growth in other parts of the system, which could lead to restricted flow in the tubes. Generally, however, SPR holds potential as a biofilm model system, as it shows properties ideal for *in vitro* models: uniform biofilm formation, uniform reproducibility and the ability to be investigated quantitatively (Yasuda, Koga & Fukuoka, 1999).

8 Conclusion

The aim of this study was to compare CLSM and SPR as *in vitro* biofilm models and to evaluate mesoporous silica nanoparticles effect on *E. coli* and *S. aureus* biofilms. Due to the complexity and variety of biofilms, adequate *in vitro* biofilm models are hard to achieve. The main takeaway of this study is that the growth of biofilms will vary greatly depending on the different conditions. SPR, however, shows great promise as a biofilm model as it provides quantitative results on every stage of the biofilm lifecycle. More information about the biofilm formation pattern in a SPR system is needed for greater reproducibility of the results. In addition, the fate of nanoparticles in biofilms needs to be more closely investigated, including the formation of biomolecular corona and its effect on the function of the nanoparticles. The interactions between mesoporous silica nanoparticles and bacteria needs to be evaluated, including possible toxic effects on microbial cells. Overall, mesoporous silica nanoparticles show great potential as anti-biofilm agents due to their tunability for pharmaceutical purposes and their ability to penetrate through the extracellular matrix.

9 Summary in Swedish – Svensk sammanfattning

9.1 Bakgrund

Ett av de största hoten mot global hälsa idag är bakteriers resistens mot antibiotika (World Health Organization, 2018). Medan antibiotika är effektiv mot fria planktoniska bakterier, har det visat sig att de flesta bakterier i naturen förekommer i kluster av bakterier fästa vid en yta omgiven av extracellulära substanser. Denna form kallas biofilm, och kan vara upp till tusen gånger mer resistent mot antimikrobiella medel än fria bakterier (Ceri *et al*., 1999). Det nationella hälsoinsistutet i USA (National Institute of Health) (2002) räknar med att 80% av mikrobiella infektioner i människan är kopplade till biofilmer. Biofilmer har kopplats till infektioner såsom parodontit och infektioner hos patienter med cystisk fibros, och kan formas på en mängd medicinska produkter såsom endotrakealtuber, mekaniska hjärtklaffar, pacemakers, ledproteser och urinkatetrar (Donlan 2001, 2002). Biofilmers unika egenskaper fås av den extracellulära matrisen, som uppgår till 90% av den torra massan (Flemming & Wingender, 2010). Den extracellulära matrisen består av cellproducerade substanser (EPS) såsom polysackarider, proteiner och extracellulär DNA. Upp till 97% av den extracellulära matrisen kan bestå av vatten, och vissa biofilmer har visats innehålla vattenkanaler för enkel distribution av näringsämnen och syre (Stoodley, Debeer & Lewandowski, 1994; Zhang, Bishop & Kupferle, 1998). Den extracellulära matrisen agerar som en skyddande barriär och hindrar penetration av antimikrobiella ämnen (Mah & O'Toole, 2001). Biofilmernas begränsade tillgång till syre och näringsämne gör att bakterierna kommer att befinna sig i olika stadier av tillväxt (Stewart & Franklin, 2008). Förutom heterogenitet kan genetisk variation också förekomma, vilket bidrar till biofilmers resistens mot antimikrobiella ämnen (Flemming & Wingender, 2010).

Flera metoder för att överkomma biofilmers resistens har föreslagits. Nanopartiklar, vars storlek på en nanometerskala tillåter penetration genom biologiska membraner, är en av dem (Hosokawa 2012). Mesoporösa kiseldioxidpartiklar (MSN:er) har lovande egenskaper för administrationen av läkemedelssubstanser in i biofilmer. Dessa egenskaper inkluderar såväl kontrollerbar partikelstorlek, morfologi och porösitet som kemisk stabilitet (Slowing *et al*., 2007). Silanol-grupperna på ytan möjliggör modifiering av nanopartiklarnas kemiska egenskaper genom ytfunktionalisering (Vallet-Regí, 2006). MSN:er impregnerade med antimikrobiella ämnen såsom klorhexidin och levofloxacin har visats ha större effekt på

biofilmer jämfört med den fria antimikrobiella substansen (Álvares *et al*., 2022; Li *et al*., 2016).

En utmaning med utvecklingen av anti-biofilm substanser är *in vitro*-modellers begränsade förmåga att representera biofilmers komplexitet. Användningen av ytplasmonresonansbiosensor (SPR) för biofilmer är en relativt ny metod. SPR möjliggör känslig mätning av kinetik och affinitet för biomolekylära bindningar i realtid (Singh, 2016). SPR baserar sig på accelerationen av ytplasmoner som finns på ytan av en metall (Bakhtiar, 2013). När en p-polariserad ljusstråle under bestämda förhållanden helt reflekteras av en yta uppstår en total intern reflektion. När detta inträffar mellan två icke-absorberande medier, läcker en viss elektrisk intensitet som kallas det evanescenta fältet in i det andra icke-absorberande mediet. Den evanescenta vågen exciterar elektroner på en metallyta som är i kontakt med det icke-absorberande mediet, vilket får dem att resonera. Dessa resonerande elektroner, som kallas ytplasmoner, är känsliga för förändringar på metallytan och i den omgivande miljön. Förändringar i massan på sensorns yta detekteras som en förändring i resonansvinkeln. SPR kan därför registrera bakterier och EPS inom det evanescenta fältet (Zhang *et al*., 2018)

I denna studie syntetiserades mesoporösa kiseldioxidpartiklar av två olika former, sfärer (MSP) och stavar (MSR). En del av partiklarna funktionaliserades med polyetylenimin (PEI) för att ge dem en positiv ytladdning (PEI-MSP och PEI-MSR). Partiklarnas penetration av *Staphylococcus aureus* och *Escherichia coli* biofilmer undersöktes med hjälp av konfokal mikroskopi. Effekten av MSP och PEI-MSP på *E. coli* biofilm undersöktes även med hjälp av SPR.

9.2 Material och metoder

Syntesen av MSP baserades på protokollet beskrivet av Desai *et al*. (2014). Syntetiseringsprocessen går ut på att ett ytaktivt ämne, CTAB, självaggregerar till miceller och kiseldioxiden formar en vägg runt micellerna genom att kondensera runt det polära området (figur 2). Därefter utförs extraktion för att avlägsna CTAB. Partiklarna märktes med fluoresceinisotiocyanat (FITC). MSR syntetiserades enligt protokollet beskrivet av Zhao *et al*. (2017), där variationen av stavarnas längd baserades på olika volymer av $NH_3 \cdot H_2O$-lösning. Korta stavar (3 ml $NH_3 \cdot H_2O$-lösning) användes för att testa penetrationen av biofilmer. Partiklarna funktionaliserades med PEI enligt protokollet beskrivet av Desai *et al*.

(2016). Partiklarnas storlek och laddning bestämdes med hjälp av dynamisk ljusspridning (DLS) och ζ-potentialmätningar. Transmissionselektronmikroskop (TEM) användes för att bestämma storleken och formen på partiklarna.

För konfokalmikroskopi startades en planktonisk bakteriekultur i mediet och lämnades att stå över natten. Kulturen späddes ut till 0,01% och tillsattes i glasbottnade cellodlingsskålar. Kulturen fick växa i 24 timmar, varefter media avlägsnades och biofilmen sköljdes med fosfatbuffrad saltlösning (PBS). Nanopartiklar suspenderade i media sattes till och lämnades i 24 timmar, varefter biofilmen sköljdes igen och fixerades med 4% formaldehydlösning. För SPR formades biofilmen på en guldpläterad sensor. En planktonisk bakterielösning späddes ut på samma sätt som för konfokalmikroskopi. För mätningen var temperaturen 37 °C och flödeshastigheten 50 µL/minut. Först pumpades enbart medium igenom för att få en baskurva. Därefter injicerades den utspädda bakteriekulturen i 30 minuter, och biofilmen fick växa i 24 timmar. Partiklar suspenderade i media injicerades i 10 minuter, och mätningen fortsatte i minst 24 timmar.

9.3 Resultat och diskussion

De producerade sfärerna hade en diameter på 163,1 ± 17,0 nm, och stavarna en längd på 131,5 ± 30,7 nm och en bredd på 57,7 ± 9,4 nm (figur 7). Efter funktionalisering hade de en laddning på 12,3 ± 0,8 mV och 24,5 ± 1,1 mV (figur 6).

För *S. Aureus* verkade nanopartiklarna ha en negativ verkan på formationen av biofilm, eftersom det var en stor skillnad mellan biofilmen i kontroll och den innehållande nanopartiklar (figur 9). Nanopartiklarna befann sig också främst utanför de bildade mikrokolonierna av bakterier. I *E. Coli* fanns det mindre skillnad mellan kontroll och test, men bildningen av biofilmen var väldigt ojämn (figur 11). Det var också betydligt färre nanopartiklar kvar i dessa biofilmer. De partiklar som kunde ses verkade i nära kontakt med bakterieceller, vilket föreslår interaktion med cellerna i stället för extracellulära substanser. I SPR visades en ökning i massa på sensorns yta efter ungefär 2 timmar, och en ändring i intensiteten av det reflekterade ljuset under samma tid. En sänkning av kurvan efter fem timmar indikerar produktion av extracellulära substanser och formationen av en jämn biofilm (figur 13). Efter 24 timmar hade en tjock biofilm i mikrometerskala formats, som kan ses som extra toppar i vinkelspektrat. För de negativt laddade partiklarna kunde ingen större förändring ses efter injicering. Däremot kunde en stigning ses efter injicering av PEI

funktionaliserade partiklar (figur 14B). Detta indikerar att partiklar ackumulerades i biofilmen. För båda partiklarna skedde det en ändring i vinkelspektrat (figur 15), vilket indikerar att nanopartiklarna skulle kunna påverka biofilmen på en mikrometerskala.

I denna studie verkade MSN ha en negativ effekt på *S. Aureus*-biofilm i konfokalmikroskopi och *E. Coli*-biofilm i SPR. Även om MSN:er generellt anses vara säkra, finns det mycket få studier om deras mikrobiella toxicitet. Mikrobiell toxicitet av MSN:er har blivit kopplad till kvarvarande CTAB i MSN, en mindre diameter och positiv laddning (Son & Lee 2021, Mathelié-Guinlet *et al*., 2017). Partiklarnas penetrationsförmåga i konfokalmikroskopin var svår att avgöra, eftersom endast ett tunt lager av en biofilm hade bildats. Speciellt för *E. Coli* skulle det vara fördelaktigt att använda ett protokoll med en längre tillväxtperiod. I SPR verkade endast de positivt laddade partiklarna kunna penetrera *E. Coli*-biofilm.

De två olika systemen som användes för att växa biofilm i denna studie är väldigt olika. För det första växte bakterierna på två olika sorters ytor (metall och glas), vilket kan påverka både bakteriers förmåga att fästa sig samt den bildade biofilmens arkitektur (Mitik-Dineva *et al*., 2008). De två systemen kan också klassificeras som slutna och öppna. I ett slutet system (konfokalmikroskopi) ersätts media med ett visst tidsintervall, och däremellan kommer tillgängligheten av näring och ansamlingen av avfall, metaboliska biprodukter och döda celler att påverka formationen av biofilmen (Lebeaux *et al*., 2013). I ett öppet system (SPR) ersätts media hela tiden via en pump, men ett kontinuerligt flöde orsakar också belastning för biofilmen och påverkar biofilmens arkitektur (Teodósio *et al*., 2011). Som biofilmsmodell kommer ett dynamiskt system närmare i att representera kliniska infektioner, där bakterier måste stå emot flödet i blodkärlen (Grubb *et al*., 2009).

System för biofilmmodeller måste vara kontrollerbara, konstanta och reproducerbara (Lüdecke *et al*., 2014). SPR-mätningar är mycket känsliga och ger möjlighet att mäta biofilmbildning i realtid. Några begränsningar i systemet är att det är tidskrävande (antalet mätningar är begränsat till antalet flödeskanaler), uppkomsten av luftbubblor som stör mätningen och kontaminering av systemet med bakterier. SPR mäter den ackumulerade massan på sensorytan, men ger ingen information om kvaliteten på biofilmen. Som biofilmmodell för antibakteriella komponenter är den inte lämplig eftersom dödandet av bakterier fortfarande kan lämna efter sig andra komponenter av biofilmen (Koo *et al*., 2017). Men generellt sett har SPR potential som ett biofilmmodellsystem eftersom det visar egenskaper som är idealiska för *in vitro*-modeller: enhetlig biofilmbildning, enhetlig

reproducerbarhet och förmågan att undersökas kvantitativt (Yasuda, Koga & Fukuoka, 1999).

10 References

Abadian, P. N., Tandogan, N., Jamieson, J. J. & Goluch, E. D. (2014). Using surface plasmon resonance imaging to study bacterial biofilmsa. *Biomicrofluidics*, 8(2), 021804-1 - 021804-11.

Abbasi, R., Mousa, R., Dekel, N., Amartely, H., Danieli, T., Lebendiker, M., Levi-Kalisman, Y., Shalev, D. E., Metanis, N., & Chai, L. (2018). The bacterial extracellular matrix protein Tapa is a two-domain partially disordered protein. *ChemBioChem: a European journal of chemical biology*, *20*(3), 355–359.

Adams, I. L. & McLean, R. J. C. (1999). Impact of rpoS deletion on *Escherichia coli* biofilms. *Applied and environmental microbiology, 65*(9), 4285-4287.

Al-Bakri, A. G., Gilbert, P. & Allison, D. G. (2005). Influence of gentamicin and tobramycin on binary biofilm formation by co-cultures of Burkholderia cepacia and Pseudomonas aeruginosa. *Journal of basic microbiology, 45*(5), 392-396.

Allegrucci, M. & Sauer, K. (2007). Characterization of Colony Morphology Variants Isolated from Streptococcus pneumoniae Biofilms. *The Journal of Bacteriology 189*(5): 2030.

Álvarez, E., Estévez, M., Gallo-Cordova, A., González, B., Castillo, R. R., Morales, M. del, Colilla, M., Izquierdo-Barba, I., & Vallet-Regí, M. (2022). Superparamagnetic iron oxide nanoparticles decorated mesoporous silica Nanosystem for combined antibiofilm therapy. Pharmaceutics, 14(1), 163.

An, Y. H. & Friedman, R. J. (1998). Concise review of mechanisms of bacterial adhesion to biomaterial surfaces. *Journal of Biomedical Materials Research, 6*(4), 338-348.

Anderson, M. T., Martin, J. E., Odinek, J. G., & Newcomer, P. P. (1998). Effect of methanol concentration on CTAB micellization and on the formation of surfactant-templated silica (STS). *Chemistry of Materials*, *10*(6), 1490–1500.

Anwar, H., Strap, J. L., & Costerton, J. W. (1992). Establishment of aging biofilms: Possible mechanism of bacterial resistance to antimicrobial therapy. *Antimicrobial Agents and Chemotherapy*, *36*(7), 1347–1351.

Bakhtiar, R. (2013). Surface Plasmon Resonance Spectroscopy: A Versatile Technique in a Biochemist's Toolbox. *Journal of chemical education, 90*(2), 203-209.

Balaban, N., Cirioni, O., Giacometti, A., Ghiselli, R., Braunstein, J. B., Silvestri, C., Mocchegiani, F., Saba, V., & Scalise, G. (2007). Treatment of staphylococcus aureus biofilm infection by the Quorum-Sensing Inhibitor Rip. *Antimicrobial Agents and Chemotherapy*, *51*(6), 2226–2229.

Balaban, N., Giacometti, A., Cirioni, O., Gov, Y., Ghiselli, R., Mocchegiani, F., Viticchi, C., Del Prete, M. S., Saba, V., Scalise, G., & Dell'Acqua, G. (2003). Use of the Quorum-Sensing Inhibitor RNAIII-Inhibiting Peptide to Prevent Biofilm Formation In Vivo by Drug-Resistant Staphylococcus epidermidis. *The Journal of infectious diseases, 187*(4), 625-630.

Barnhart, M.M. & Chapman, M.R. (2006). Curli biogenesis and function. *Annual review of microbiology, 60*(1), 131-147.

Barran-Berdon, A. L., Ocampo, S., Haider, M., Morales-Aparicio, J., Ottenberg, G., Kendall, A., Yarmola, E., Mishra, S., Long, J. R., Hagen, S. J., Stubbs, G., & Brady, L. J. (2020). Enhanced purification coupled with biophysical analyses shows cross-β structure as a core building block for streptococcus mutans functional amyloids. *Scientific Reports*, *10*(1).

Bertani, I. & Venturi, V. (2004). Regulation of the N-Acyl Homoserine Lactone-Dependent Quorum-Sensing System in Rhizosphere Pseudomonas putida WCS358 and Cross-Talk with the Stationary-Phase RpoS Sigma Factor and the Global Regulator GacA. *Applied and Environmental Microbiology, 70*(9), 5493-5502.

Bjarnsholt, T. (2013). The role of bacterial biofilms in chronic infections. *APMIS : acta pathologica, microbiologica et immunologica Scandinavica*, 121(s136), 1-58.

Borriello, G., Werner, E., Roe, F., Kim, A. M., Ehrlich, G. D. & Stewart, P. S. (2004). Oxygen Limitation Contributes to Antibiotic Tolerance of Pseudomonas aeruginosa in Biofilms. *Antimicrobial Agents and Chemotherapy, 48*(7), 2659-2664.

Bradshaw, D. J., Marsh, P. D., Watson, G. K., & Allison, C. (1997). Oral anaerobes cannot survive oxygen stress without interacting with facuitative/aerobic species as a microbial commmunity. *Letters in Applied Microbiology*, *25*(6), 385–387.

Branda, S. S., Chu, F., Kearns, D. B., Losick, R. & Kolter, R. (2006). A major protein component of the Bacillus subtilis biofilm matrix. *Molecular microbiology, 59*(4), 1229-1238.

Branda, S. S., Vik, Å., Friedman, L. & Kolter, R. (2005). Biofilms: The matrix revisited. *Trends in microbiology (Regular ed.), 13*(1), 20-26.

Bullitt, E. & Makowski, L. (1995). Structural polymorphism of bacterial adhesion pili. *Nature (London), 373*(6510), 164-167.

Burmølle, M., Webb, J. S., Rao, D., Hansen, L. H., Sørensen, S. J., & Kjelleberg, S. (2006). Enhanced biofilm formation and increased resistance to antimicrobial agents and bacterial invasion are caused by synergistic interactions in multispecies biofilms. *Applied and Environmental Microbiology*, *72*(6), 3916–3923.

Cai, Q., Luo, Z.-S., Pang, W.-Q., Fan, Y.-W., Chen, X.-H., & Cui, F.-Z. (2001). Dilute solution routes to various controllable morphologies of MCM-41 silica with a basic medium. *Chemistry of Materials*, *13*(2), 258–263.

Canovi, M., Lucchetti, J., Stravalaci, M., Re, F., Moscatelli, D., Bigini, P., Salmona, M., & Gobbi, M. (2012). Applications of surface plasmon resonance (SPR) for the characterization of nanoparticles developed for biomedical purposes. *Sensors (Basel, Switzerland),* 12(12), 16420–16432.

Cascioferro, S., Totsika, M. & Schillaci, D. (2014). Sortase A: An ideal target for anti-virulence drug development. *Microbial pathogenesis, 77*, 105-112.

Ceri, H., Olson, M. E., Stremick, C., Read, R. R., Morck, D. & Buret, A. (1999). The Calgary Biofilm Device: New Technology for Rapid Determination of Antibiotic Susceptibilities of Bacterial Biofilms. *Journal of Clinical Microbiology 37*(6): 1771.

Chellat, M. F., Raguž, L. & Riedl, R. (2016). Targeting Antibiotic Resistance. *Angewandte Chemie International Edition* 55(23): 6600-6626.

Chen, L. & Wen, Y. (2011). The role of bacterial biofilm in persistent infections and control strategies. *International journal of oral science, 3*(2), 66-73.

Chen, Y., Ma, T., & Li T-F. (2021). Surface plasmon resonance sensing in cell biology and drug discovery. In *Surface Plasmon Resonance in Bioanalysis*. Elsevier. Edited by You-Peng Chen, Teng-Fei Ma. Volume 95, Pages 1-53

Chen, Z., Li, X., He, H., Ren, Z., Liu, Y., Wang, J., Li, Z., Shen, G. & Han, G. (2012). Mesoporous silica nanoparticles with manipulated microstructures for drug delivery. *Colloids and Surfaces B: Biointerfaces* 95: 274-278.

Christensen, B. B., Haagensen, J. A. J., Heydorn, A. & Molin, S. (2002). Metabolic Commensalism and Competition in a Two-Species Microbial Consortium. *Applied and Environmental Microbiology, 68*(5), 2495-2502.

Cloete, T. & Jacobs, L. (2001). Surfactants and the attachment of Pseudomonas aeruginosa to 3CR12 stainless steel and glass. *Water S. A., 27*(1), 21-26.

Collinson, S. K., Emödy, L., Müller, K. H., Trust, T. J., & Kay, W. W. (1991). Purification and characterization of thin, aggregative fimbriae from salmonella enteritidis. *Journal of Bacteriology*, *173*(15), 4773–4781.

Colvin, K. M., Irie, Y., Tart, C. S., Urbano, R., Whitney, J. C., Ryder, C., Howell, P. L., Wozniak, D. J., & Parsek, M. R. (2011). The Pel and PSL polysaccharides provide pseudomonas aeruginosa structural redundancy within the biofilm matrix. *Environmental Microbiology,* 14(8), 1913–1928.

Crusz, S. A., Popat, R., Rybtke, M. T., Cámara, M., Givskov, M., Tolker-Nielsen, T., Diggle, S. P., & Williams, P. (2012). Bursting the bubble on bacterial biofilms: A flow cell methodology. *Biofouling (Chur, Switzerland)*, *28*(8), 835–842.

Cucarella, C., Solano, C., Valle, J., Amorena, B., Lasa, I. & Penadés, J. R. (2001). Bap, a Staphylococcus aureus Surface Protein Involved in Biofilm Formation. *Journal of Bacteriology, 183*(9), 2888-2896.

Davies, D. G. & Marques C. N. (2009). A fatty acid messenger is responsible for inducing dispersion in microbial biofilms. *Journal of Bacteriology*, *191*(5), 1393–1403.

Desai, D., Karaman, D. S., Prabhakar, N., Tadayon, S., Duchanoy, A., Toivola, D. M., Rajput, S., Näreoja, T. & Rosenholm, J. M. (2014). Design considerations for mesoporous silica nanoparticulate systems in facilitating biomedical applications. *Open Material Sciences1*(1): 16-43.

Desai, D., Prabhakar, N., Mamaeva, V., Sen Karaman, D., Lähdeniemi, I., Sahlgren, C., Rosenholm, J. & Toivola, D. (2016). Targeted modulation of cell differentiation in distinct regions of the gastrointestinal tract via oral administration of differently peg-Pei functionalized mesoporous silica nanoparticles. *International Journal of Nanomedicine*, 11, 299-313.

Devlin, H., Fulaz, S., Hiebner, D. W., O'Gara, J. P. & Casey, E. (2021). Enzyme-Functionalized Mesoporous Silica Nanoparticles to Target Staphylococcus aureus and Disperse Biofilms. *International journal of nanomedicine, 16*, 1929-1942.

Diggle, S. P., Cornelis, P., Williams, P. & Cámara, M. (2006). 4-Quinolone signalling in Pseudomonas aeruginosa: Old molecules, new perspectives. *International journal of medical microbiology, 296*(2), 83-91.

Doadrio, A., Sousa, E., Doadrio, J., Pérez Pariente, J., Izquierdo-Barba, I. & Vallet-Regí, M. (2004). Mesoporous SBA-15 HPLC evaluation for controlled gentamicin drug delivery. *Journal of Controlled Release 97*(1): 125-132.

Docter, D., Westmeier, D., Markiewicz, M., Stolte, S., Knauer, S. K. & Stauber, R. H. (2015). The nanoparticle biomolecule corona: Lessons learned - challenge accepted? *Chemical Society reviews, 44*(17), 694-6121.

Donlan, R. (2001). Biofilms and Device-Associated Infections. *Emerging Infectious Diseases 7*(2): 277-281.

Donlan, R. (2002). Biofilms: Microbial life on surfaces. *Emerging Infectious Diseases* 8(9): 881-890.

Dudak, F. C. & Boyacı, İ. H. (2009). Rapid and label-free bacteria detection by surface plasmon resonance (SPR) biosensors. *Biotechnology journal, 4*(7), 1003-1011.

Dueholm, M. S., Petersen, S. V., Sønderkaer, M., Larsen, P., Christiansen, G., Hein, K. L., Enghild, J. J., Nielsen, J. L., Nielsen, K. L., Nielsen, P. H., & Otzen, D. E. (2010). Functional amyloid in pseudomonas. *Molecular Microbiology*. *77*(4), 1009-1020.

Eckert, R., Qi, F., Yarbrough, D. K., He, J., Anderson, M. H., & Shi, W. (2006). Adding selectivity to antimicrobial peptides: Rational design of a multidomain peptide against *pseudomonas* spp. *Antimicrobial Agents and Chemotherapy*, *50*(4), 1480–1488.

Elias, S. & Banin, E. (2012). Multi-species biofilms: Living with friendly neighbors. FEMS microbiology reviews, 36(5), 990-1004.

Fallarero, A., Skogman, M., Kujala, J., Rajaratnam, M., Moreira, V. M., Yli-Kauhaluoma, J. & Vuorela, P. (2013). (+)-Dehydroabietic acid, an abietane-type diterpene, inhibits Staphylococcus aureus biofilms in vitro. *International journal of molecular sciences, 14*(6), 12054-12072.

Ferry, J. L., Craig, P., Hexel, C., Sisco, P., Frey, R., Pennington, P. L., Fulton, M. H., Scott, I. G., Decho, A. W., Kashiwada, S., Murphy, C. J., & Shaw, T. J. (2009). Transfer of gold nanoparticles from the water column to the Estuarine Food Web. *Nature Nanotechnology*, 4(7), 441–444.

, H., Neu, T. R. & Wingender, J. (2017). *The perfect slime: Microbial extracellular polymeric substances (EPS)*. IWA Publishing.

Flemming, H., Neu, T. R. & Wozniak, D. J. (2007). The EPS matrix: The "house of biofilm cells". *Journal of bacteriology, 189*(22), 7945-7947.

Flemming, H. & Wingender, J. (2010). The biofilm matrix. *Nature Reviews Microbiology* 8(9): 623.

Fletcher, M. & Loeb, G. I. (1979). Influence of Substratum Characteristics on the Attachment of a Marine Pseudomonad to Solid Surfaces. *Applied and Environmental Microbiology, 37*(1), 67-72.

Fouladkhah, A., Geornaras, I. & Sofos, J. N. (2013). Biofilm Formation of O157 and Non-O157 Shiga Toxin-Producing *Escherichia coli* and Multidrug-Resistant and Susceptible *Salmonella Typhimurium* and Newport and Their Inactivation by Sanitizers. *Journal of food science, 78*(6), M880-M886.

Fulaz, S., Vitale, S., Quinn, L. & Casey, E. (2019). Nanoparticle–Biofilm Interactions: The Role of the EPS Matrix. *Trends in microbiology (Regular ed.), 27*(11), 915-926.

Gjermansen, M., Ragas, P., Sternberg, C., Molin, S. & Tolker-Nielsen, T. (2005). Characterization of starvation-induced dispersion in Pseudomonas putida biofilms. *Environmental microbiology, 7*(6), 894-904.

Golberg, K., Emuna, N., Vinod, T. P., van Moppes, D., Marks, R. S., Arad, S. M., & Kushmaro, A. (2016). Anti-Biofilms: Novel Anti-Adhesive biomaterial patches: Preventing biofilm with Metal Complex Films (MCF) derived from a microalgal polysaccharide (adv. mater. interfaces 9/2016). *Advanced Materials Interfaces*, *3*(9).

Goulter, R. M., Gentle, I. R. & Dykes, G. A. (2010). Characterisation of Curli Production, Cell Surface Hydrophobicity, Autoaggregation and Attachment Behaviour of Escherichia coli O157. *Current microbiology, 61*(3), 157-162.

Grover, N., Plaks, J. G., Summers, S. R., Chado, G. R., Schurr, M. J. & Kaar, J. L. (2016). Acylase-containing polyurethane coatings with anti-biofilm activity: Acylase-Containing Anti-Biofilm Coatings. *Biotechnology and bioengineering, 113*(12), 2535-2543.

Grubb, S. E. W., Murdoch, C., Sudbery, P. E., Saville, S. P., Lopez-Ribot, J. L. & Thomhill, M. H. (2009). Adhesion of Candida albicans to Endothelial Cells under Physiological Conditions of Flow. *Infection and Immunity, 77*(9), 3872-3878.

Gupta, T. T., Gupta, N. K., Burback, P. & Stoodley, P. (2021). Free-Floating Aggregate and Single-Cell-Initiated Biofilms of Staphylococcus aureus. *Antibiotics (Basel), 10*(8), 889.

Guttula, D., Yao, M., Baker, K., Yang, L., Goult, B. T., Doyle, P. S. & Yan, J. (2019). Calcium-mediated Protein Folding and Stabilization of Salmonella Biofilm-associated Protein A. *Journal of molecular biology, 431*(2), 433-443.

Hajipour, M. J., Fromm, K. M., Akbar Ashkarran, A., Jimenez de Aberasturi, D., Larramendi, I. R., Rojo, T., Serpooshan, V., Parak, W. J., & Mahmoudi, M. (2012). Antibacterial properties of nanoparticles. T*rends in Biotechnology*, 30(10), 499–511.

Harmsen, M., Lappann, M., Knøchel, S. & Molin, S. (2010). Role of Extracellular DNA during Biofilm Formation by Listeria monocytogenes. *Applied and Environmental Microbiology, 76*(7), 2271-2279.

He, J., Anderson, M. H., Shi, W. & Eckert, R. (2009). Design and activity of a 'dual-targeted' antimicrobial peptide. *International journal of antimicrobial agents, 33*(6), 532-537.

He, Q., Shi, J., Chen, F., Zhu, M. & Zhang, L. (2010). An anticancer drug delivery system based on surfactant-templated mesoporous silica nanoparticles. *Biomaterials, 31*(12), 3335-3346.

He, Q., Zhang, Z., Gao, F., Li, Y. & Shi, J. (2011). In vivo biodistribution and urinary excretion of mesoporous silica nanoparticles: Effects of particle size and PEGylation. *Small 7*(2): 271.

He, Q., Zhang, Z., Gao, Y., Shi, J. & Li, Y. (2009). Intracellular localization and cytotoxicity of spherical mesoporous silica nano-and microparticles. *Small 5*(23): 2722-2729.

Hinsa, S. M., Espinosa-Urgel, M., Ramos, J. L. & O'Toole, G. A. (2003). Transition from reversible to irreversible attachment during biofilm formation by Pseudomonas fluorescens WCS365 requires an ABC transporter and a large secreted protein. *Molecular microbiology, 49*(4), 905-918.

Hobley, L., Ostrowski, A., Rao, F. V., Bromley, K. M., Porter, M., Prescott, A. R., MacPhee, C. E., van Aalten, D. M. F. & Stanley-Wall, N. R. (2013). BslA is a self-assembling bacterial hydrophobin that coats the Bacillus subtilis biofilm. *Proceedings of the National Academy of Sciences - PNAS, 110*(33), 13600-13605.

Hoffman, L. R., Déziel, E., D'Argenio, D. A., Lépine, F., Emerson, J., McNamara, S., Gibson, R. L., Ramsey, B. W., & Miller, S. I. (2006). Selection for *Staphylococcus aureus* small-colony variants due to growth in the presence of *Pseudomonas aeruginosa*. *Proceedings of the National Academy of Sciences*, *103*(52), 19890–19895.

Hong, W., Nyaruaba, R., Li, X., Liu, H., Yang, H. & Wei, H. (2021). In-situ and Real-Time Monitoring of the Interaction Between Lysins and Staphylococcus aureus Biofilm by Surface Plasmon Resonance. *Frontiers in microbiology, 12*, 783472.

Hosokawa, M. (2012). *Nanoparticle technology handbook* (2nd ed.). Elsevier. Retrieved from https://ebookcentral.proquest.com/lib/abo-ebooks/reader.action?docID=892235

Howlin, R. P., Cathie, K., Hall-Stoodley, L., Cornelius, V., Duignan, C., Allan, R. N., Fernandez, B. O., Barraud, N., Bruce, K. D., Jefferies, J., Kelso, M., Kjelleberg, S., Rice, S. A., Rogers, G. B., Pink, S., Smith, C., Sukhtankar, P. S., Salib, R., Legg, J. & Webb, J. S. (2017). Low-dose nitric oxide as targeted

anti-biofilm adjunctive therapy to treat chronic pseudomonas aeruginosa infection in cystic fibrosis. *Molecular Therapy*, 25(9), 2104–2116.

Hu, P., Huang, P. & Chen, M. W. (2013). Curcumin reduces Streptococcus mutans biofilm formation by inhibiting sortase A activity. *Archives of oral biology, 58*(10), 1343-1348.

Huang, X. Li, L., Liu, T., Hao, N., Liu, H., Chen, D. & Tang, F. (2011). The shape effect of mesoporous silica nanoparticles on biodistribution, clearance, and biocompatibility in vivo. *ACS Nano 5*(7): 5390-5399.

Huh, A. J. & Kwon, Y. J. (2011). "Nanoantibiotics": A new paradigm for treating infectious diseases using nanomaterials in the antibiotics resistant era. *Journal of Controlled Release,156*(2): 128-145.

Huh, S., Wiench, J. W., Yoo, J., Pruski, M. & Lin, V. S. (2003). Organic Functionalization and Morphology Control of Mesoporous Silicas via a Co-Condensation Synthesis Method. *Chemistry of materials, 15*(22), 4247-4256.

Hymes, S. R., Randis, T. M., Sun, T. Y., & Ratner, A. J. (2013). DNase inhibits Gardnerella vaginalis biofilms in vitro and in vivo. *The Journal of Infectious Diseases*, *207*(10), 1491–1497.

Ikuma, K., Decho, A. W. & Lau, B. L. T. (2015). When nanoparticles meet biofilms-interactions guiding the environmental fate and accumulation of nanoparticles. *Frontiers in microbiology, 6*, 591.

Ito, A., Taniuchi, A., May, T., Kawata, K. & Okabe, S. (2009). Increased Antibiotic Resistance of Escherichia coli in Mature Biofilms. *Applied and Environmental Microbiology, 75*(12), 4093-4100.

Itoh, Y., Wang, X., Hinnebusch, B. J., Preston, J. F. & Romeo, T. (2005). Depolymerization of β-1,6-N-Acetyl-d-Glucosamine Disrupts the Integrity of Diverse Bacterial Biofilms. *Journal of Bacteriology, 187*(1), 382-387.

Izano, E. A., Amarante, M. A., Kher, W. B. & Kaplan, J. B. (2008). Differential Roles of Poly-N-Acetylglucosamine Surface Polysaccharide and Extracellular DNA in Staphylococcus aureus and Staphylococcus epidermidis Biofilms. *Applied and Environmental Microbiology, 74*(2), 470-476.

Jakubovics, N. & Kolenbrander, P. (2010). The road to ruin: The formation of disease-associated oral biofilms. *Oral diseases, 16*(8), 729-739.

Jenkins, A. T. A., ffrench-constant, R., Buckling, A., Clarke, D. J. & Jarvis, K. (2004). Study of the Attachment of Pseudomonas aeruginosa on Gold and Modified Gold Surfaces Using Surface Plasmon Resonance. *Biotechnology progress, 20*(4), 1233-1236.

Jijie, R., Barras, A., Teodorescu, F., Boukherroub, R. & Szunerits, S. (2017). Advancements on the molecular design of nanoantibiotics: Current level of development and future challenges. *Molecular Systems Design & Engineering,2*(4): 349-369.

Kaasalainen, M., Aseyev, V., von Haartman, E., Karaman, D. Ş., Mäkilä, E., Tenhu, H., Rosenholm, J., & Salonen, J. (2017). Size, stability, and porosity of mesoporous nanoparticles characterized with light scattering. *Nanoscale Research Letters*, 12(1).

Karatan, E. & Watnick, P. (2009). Signals, Regulatory Networks, and Materials That Build and Break Bacterial Biofilms. *Microbiology and Molecular Biology Reviews*, 73(2), 310-347.

Kim, S. Y., Lee, S. E., Kim, Y. R., Kim, C. M., Ryu, P. Y., Choy, H. E., Chung, S. S., & Rhee, J. H. (2003). Regulation of vibrio vulnificus virulence by the luxs quorum-sensing system. *Molecular Microbiology*, 48(6), 1647–1664.

Kirisits, M. J., Prost, L., Starkey, M. & Parsek, M. R. (2005). Characterization of Colony Morphology Variants Isolated from Pseudomonas aeruginosa Biofilms. *Applied and Environmental Microbiology 71*(8): 4809.

Koo, H., Allan, R. N., Howlin, R. P., Stoodley, P. & Hall-Stoodley, L. (2017). Targeting microbial biofilms: Current and prospective therapeutic strategies. *Nature reviews. Microbiology, 15*(12), 740-755.

Korber, D. R., Lawrence, J. R., Sutton, B. & Caldwell, D. E. (1989). Effect of laminar flow velocity on the kinetics of surface recolonization by Mot+ and Mot- Pseudomonas fluorescens. *Microbial ecology, 18*(1), 1-19.

Kuboniwa, M., Tribble, G. D., James, C. E., Kilic, A. O., Tao, L., Herzberg, M. C., . . . Lamont, R. J. (2006). Streptococcus gordonii utilizes several distinct gene functions to recruit Porphyromonas gingivalis into a mixed community. *Molecular microbiology, 60*(1), 121-139.

Lasa, I. & Penadés, J. R. (2006). Bap: A family of surface proteins involved in biofilm formation. *Research in microbiology, 157*(2), 99-107.

Lawrence, J., Neu, T. & Swerhone, G. (1998). Application of multiple parameter imaging for the quantification of algal, bacterial and exopolymer components of microbial biofilms. *Journal of microbiological methods*, 32(3), 253-261.

Lebeaux, D., Chauhan, A., Rendueles, O. & Beloin, C. (2013). From in vitro to in vivo Models of Bacterial Biofilm-Related Infections. *Pathogens (Basel), 2*(2), 288-356.

Lee, S., Yun, H.-S. & Kim, S.-H. (2011). The comparative effects of mesoporous silica nanoparticles and colloidal silica on inflammation and apoptosis. *Biomaterials* 32(35): 9434-9443.

Lemire, J. A., Harrison, J. J. & Turner, R. J. (2013). Antimicrobial activity of metals: Mechanisms, molecular targets and applications. *Nature reviews. Microbiology, 11*(6), 371-384.

Leriche, V., Briandet, R. & Carpentier, B. (2003). Ecology of mixed biofilms subjected daily to a chlorinated alkaline solution: Spatial distribution of bacterial species suggests a protective effect of one species to another. *Environmental microbiology, 5*(1), 64-71.

Leung, J. W., Liu, Y. L., Desta, T., Libby, E., Inciardi, J. F. & Lam, K. (1998). Is there a synergistic effect between mixed bacterial infection in biofilm formation on biliary stents? *Gastrointestinal endoscopy, 48*(3), 250-257.

Li, C., Ding, Y., Kuddannaya, S., Zhang, Y. & Yang, L. (2017). Anti-bacterial properties of collagen-coated glass and polydimethylsiloxane substrates. *Journal of materials science, 52*(17), 9963-9978.

Li, X., Wong, C., Ng, T., Zhang, C., Leung, K. C. & Jin, L. (2016). The spherical nanoparticle-encapsulated chlorhexidine enhances anti-biofilm efficiency through an effective releasing mode and close microbial interactions. International Journal of Nanomedicine, 11, pp. 2471-2480

Li, X., Yeh, Y., Giri, K., Mout, R., Landis, R. F., Prakash, Y. S. & Rotello, V. M. (2015). Control of nanoparticle penetration into biofilms through surface design. *Chemical communications (Cambridge, England), 51*(2), 282-285.

Liu, T., Li, L., Teng, X., Huang, X., Liu, H., Chen, D., Ren, J., He, J. & Tang, F. (2011). Single and repeated dose toxicity of mesoporous hollow silica nanoparticles in intravenously exposed mice. *Biomaterials* 32(6): 1657-1668.

Liu, W., Li, S., Wang, Z., Yan, E. C. Y. & Leblanc, R. M. (2017). Characterization of Surface-Active Biofilm Protein BslA in Self-Assembling Langmuir Monolayer at the Air–Water Interface. *Langmuir, 33*(30), 7548-7555.

López, D., Vlamakis, H. & Kolter, R. (2010). Biofilms. *Cold Spring Harbor perspectives in biology*, 2(7), a000398.

López-Ochoa, J., Montes-García, J. F., Vázquez, C., Sánchez-Alonso, P., Pérez-Márquez, V. M., Blackall, P. J., Vaca, S., & Negrete-Abascal, E. (2017). Gallibacterium elongation factor-tu possesses amyloid-like protein characteristics, participates in cell adhesion, and is present in biofilms. *Journal of Microbiology*, *55*(9), 745–752.

Lu, M., Ge, Y., Qiu, J., Shao, D., Zhang, Y., Bai, J., Zheng, X., Chang, Z., Wang, Z., Dong, W., & Tang, C. (2018). Redox/ph dual-controlled release of chlorhexidine and silver ions from biodegradable mesoporous silica nanoparticles against oral biofilms. *International Journal of Nanomedicine*, Volume 13, 7697–7709.

Lüdecke, C., Jandt, K. D., Siegismund, D., Kujau, M. J., Zang, E., Rettenmayr, M., Bossert, J., & Roth, M. (2014). Reproducible biofilm cultivation of chemostat-grown escherichia coli and investigation of bacterial adhesion on biomaterials using a non-constant-depth film fermenter. *PLoS ONE*, *9*(1).

Lund, B. & Edlund, C. (2003). Bloodstream Isolates of Enterococcus faecium Enriched with the Enterococcal Surface Protein Gene, esp, Show Increased Adhesion to Eukaryotic Cells. *Journal of Clinical Microbiology, 41*(11), 5183-5185.

Lynch, D. J., Fountain, T. L., Mazurkiewicz, J. E. & Banas, J. A. (2007). Glucan-binding proteins are essential for shaping Streptococcus mutans biofilm architecture. *FEMS microbiology letters, 268*(2), 158-165.

Maalouf, R., Fournier-Wirth, C., Coste, J., Chebib, H., Saïkali, Y., Vittori, O., Errachid, A., Cloarec, J.-P., Martelet, C., & Jaffrezic-Renault, N. (2007). Label-free detection of bacteria by electrochemical impedance spectroscopy: comparison to surface plasmon resonance. *Analytical Chemistry*, 79(13), 4879–4886.

Mah, T. C. & O'Toole, G. A. (2001). Mechanisms of biofilm resistance to antimicrobial agents. *Trends in Microbiology, 9*(1), 34-39.

Maira-Litran, T., Kropec, A., Abeygunawardana, C., Joyce, J., Mark, G. I., Goldmann, D. A. & Pier, G. B. (2002). Immunochemical Properties of the Staphylococcal Poly-N-Acetylglucosamine Surface Polysaccharide. *Infection and Immunity, 70*(8), 4433-4440.

Mathelié-Guinlet, M., Béven, L., Moroté, F., Moynet, D., Grauby-Heywang, C., Gammoudi, I., Delville, M.-H., & Cohen-Bouhacina, T. (2017). Probing the threshold of membrane damage and cytotoxicity effects induced by silica nanoparticles in escherichia coli bacteria. *Advances in Colloid and Interface Science*, 245, 81–91.

McNab, R., Ford, S. K., El-Sabaeny, A., Barbieri, B., Cook, G. S. & Lamont, R. J. (2003). LuxS-Based Signaling in Streptococcus gordonii: Autoinducer 2 Controls Carbohydrate Metabolism and Biofilm Formation with Porphyromonas gingivalis. *Journal of Bacteriology, 185*(1), 274-284.

Mitik-Dineva, N., Wang, J., Truong, V. K., Stoddart, P., Malherbe, F., Crawford, R. J. & Ivanova, E. P. (2008). Escherichia coli, Pseudomonas aeruginosa, and Staphylococcus aureus Attachment Patterns on Glass Surfaces with Nanoscale Roughness. *Current microbiology, 58*(3), 268-273.

Monopoli, M. P., Aberg, C., Salvati, A., and Dawson, K. A. (2012). Biomolecular coronas provide the biological identity of nanosized materials. *Nat. Nanotechnol.* 7, 779–786.

Nairi, V., Medda, L., Monduzzi, M. & Salis, A. (2017). Adsorption and release of ampicillin antibiotic from ordered mesoporous silica. *Journal of Colloid And Interface Science 497:* 217-225.

National Institute of Health (2002). Research on microbial biofilms: PA Number: PA-03-047. Retrieved from https://grants.nih.gov/grants/guide/pa-files/PA-03-047.html (29.03.2019).

Nel, A. E., Mädler, L., Velegol, D., Xia, T., Hoek, E. M. V., Somasundaran, P., Klaessig, F., Castranova, V. & Thompson, M. (2009). Understanding biophysicochemical interactions at the nano–bio interface. *Nature Materials* 8(7): 543.

Nguyen, D., Joshi-Datar, A., Lepine, F., Bauerle, E., Olakanmi, O., Beer, K., McKay, G., Siehnel, R., Schafhauser, J., Wang, Y., Britigan, B. E., & Singh, P. K. (2011). Active starvation responses mediate antibiotic tolerance in biofilms and nutrient-limited bacteria. *Science (American Association for the Advancement of Science),* 334(6058), 982–986.

Nirmala Grace, A. & Pandian, K. (2007). Antibacterial efficacy of aminoglycosidic antibiotics protected gold nanoparticles—A brief study. *Colloids and Surfaces A: Physicochemical and Engineering Aspects 297*(1): 63-70.

Nishimori, H., Kondoh, M., Isoda, K., Tsunoda, S., Tsutsumi, Y. & Yagi, K. (2009). Silica nanoparticles as hepatotoxicants. *European Journal of Pharmaceutics and Biopharmaceutics* 72(3): 496-501.

Oberdörster, G., Oberdörster, E. & Oberdörster, J. (2005). Nanotoxicology: An emerging discipline evolving from studies of ultrafine particles. *Environmental Health Perspectives 113*(7): 823-839.

Oli, M. W., Otoo, H. N., Crowley, P. J., Heim, K. P., Nascimento, M. M., Ramsook, C. B., Lipke, P. N., & Brady, L. J. (2012). Functional amyloid formation by streptococcus mutans. *Microbiology*, *158*(12), 2903–2916.

Olsen, N., Thiran, E., Hasler, T., Vanzieleghem, T., Belibasakis, G., Mahillon, J., Loessner, M., & Schmelcher, M. (2018). Synergistic removal of static and dynamic Staphylococcus aureus biofilms by combined treatment with a bacteriophage endolysin and a polysaccharide depolymerase. *Viruses*, *10*(8), 438.

Paczkowski, J. E., Mukherjee, S., McCready, A. R., Cong, J.-P., Aquino, C. J., Kim, H., Henke, B. R., Smith, C. D., & Bassler, B. L. (2017). Flavonoids suppress pseudomonas aeruginosa virulence through allosteric inhibition of quorum-sensing receptors. *Journal of Biological Chemistry*, *292*(10), 4064–4076.

Pamp, S. J., Sternberg, C. & Tolker-Nielsen, T. (2009). Insight into the microbial multicellular lifestyle via flow-cell technology and confocal microscopy. *Cytometry. Part A, 75A*(2), 90-103.

Paterson, G. K. & Mitchell, T. J. (2004). The biology of Gram-positive sortase enzymes. *Trends in microbiology (Regular ed.), 12*(2), 89-95.

Patti, J. M., Allen, B. L., McGavin, M. J., & Höök, M. (1994). MSCRAMM-mediated adherence of microorganisms to host tissues. *Annual Review of Microbiology*, *48*(1), 585–617.

Petrova, O. E. & Sauer, K. (2016). Escaping the biofilm in more than one way: Desorption, detachment or dispersion. *Current opinion in microbiology, 30*, 67-78.

Peulen, T. & Wilkinson, K. J. (2011). Diffusion of Nanoparticles in a Biofilm. *Environmental science & technology, 45*(8), 3367-3373.

Piras, C., Di Ciccio, P. A., Soggiu, A., Greco, V., Tilocca, B., Costanzo, N., Ceniti, C., Urbani, A., Bonizzi, L., Ianieri, A., & Roncada, P. (2021). S. aureus biofilm protein expression linked to antimicrobial resistance: A proteomic study. *Animals (Basel)*, 11(4), 966.

Purevdorj-Gage, B., Costerton, W. J. & Stoodley, P. (2005). Phenotypic differentiation and seeding dispersal in non-mucoid and mucoid Pseudomonas aeruginosa biofilms. *Microbiology (Society for General Microbiology), 151*(5), 1569-1576.

Rabin, N., Zheng, Y., Opoku-Temeng, C., Du, Y., Bonsu, E. & Sintim H.O. (2015). Biofilm formation mechanisms and targets for developing antibiofilm agents. *Future Med. Chem,* 7(4), 493–512

Ramsey, M. M. & Whiteley, M. (2009). Polymicrobial Interactions Stimulate Resistance to Host Innate Immunity through Metabolite Perception. *Proceedings of the National Academy of Sciences - PNAS, 106*(5), 1578-1583.

Ramsugit, S., Guma, S., Pillay, B., Jain, P., Larsen, M. H., Danaviah, S. & Pillay, M. (2013). Pili contribute to biofilm formation in vitro in Mycobacterium tuberculosis. *Antonie van Leeuwenhoek, 104*(5), 725-735.

Reisner, A., Haagensen, J. A. J., Schembri, M. A., Zechner, E. L. & Molin, S. (2003). Development and maturation of Escherichia coli K-12 biofilms. *Molecular microbiology, 48*(4), 933-946.

Rice, K. C., Mann, E. E., Endres, J. L., Weiss, E. C., Cassat, J. E., Smeltzer, M. S. & Bayles, K. W. (2007). The cidA Murein Hydrolase Regulator Contributes to DNA Release and Biofilm Development in Staphylococcus aureus. *Proceedings of the National Academy of Sciences - PNAS, 104*(19), 8113-8118.

Riedel, C. U., Monk, I. R., Casey, P. G., Waidmann, M. S., Gahan, C. G. M. & Hill, C. (2009). AgrD-dependent quorum sensing affects biofilm formation, invasion, virulence and global gene expression profiles in Listeria monocytogenes. *Molecular microbiology, 71*(5), 1177-1189.

Roeselers, G., Zippel, B., Staal, M., van Loosdrecht, M. & Muyzer, G. (2006). On the reproducibility of microcosm experiments – different community composition in parallel phototrophic biofilm microcosms. *FEMS microbiology ecology, 58*(2), 169-178.

Romero, D., Aguilar, C., Losick, R. & Kolter, R. (2010). Amyloid Fibers Provide Structural Integrity to Bacillus Subtilis Biofilms. *Proceedings of the National Academy of Sciences - PNAS, 107*(5), 2230-2234.

Rosemary, M. J., Maclaren, I. & Pradeep, T. (2006). Investigations of the antibacterial properties of ciprofloxacin@SiO2. *Langmuir : the ACS journal of surfaces and colloids 22*(24): 10125.

Roux, A., Beloin, C., & Ghigo, J.-M. (2005). Combined inactivation and expression strategy to study gene function under physiological conditions: Application to identification of new *escherichia coli* adhesins. *Journal of Bacteriology*, *187*(3), 1001–1013.

Rudney, J. D., Chen, R., Lenton, P., Li, J., Li, Y., Jones, R. S., Reilly, C., Fok, A. S., & Aparicio, C. (2012). A reproducible oral microcosm biofilm model for testing dental materials. *Journal of Applied Microbiology*, *113*(6), 1540–1553.

Rumbaugh, K. P. & Sauer, K. (2020). Biofilm dispersion. *Nature reviews. Microbiology, 18*(10), 571-586.

Ryan, R. P., Lucey, J., O'Donovan, K., McCarthy, Y., Yang, L., Tolker-Nielsen, T. & Dow, J. M. (2009). HD-GYP domain proteins regulate biofilm formation and virulence in Pseudomonas aeruginosa. *Environmental microbiology, 11*(5), 1126-1136.

Sae-ung, P., Wijitamornloet, A., Iwasaki, Y., Thanyasrisung, P. & Hoven, V. P. (2019). Clickable Zwitterionic Copolymer as a Universal Biofilm-Resistant Coating. *Macromolecular materials and engineering, 304*(9), 1900286.

Samuelsen, Ø., Haukland, H. H., Kahl, B. C., von Eiff, C., Proctor, R. A., Ulvatne, H., Sandvik, K., & Vorland, L. H. (2005). Staphylococcus aureus small colony variants are resistant to the antimicrobial peptide lactoferricin B. *Journal of Antimicrobial Chemotherapy*, *56*(6), 1126–1129.

Schuster, M., Lostroh, C. P., Ogi, T. & Greenberg, E. P. (2003). Identification, Timing, and Signal Specificity of Pseudomonas aeruginosa Quorum-Controlled Genes: A Transcriptome Analysis. *Journal of Bacteriology, 185*(7), 2066-2079.

Schwartz, K., Stephenson, R., Hernandez, M., Jambang, N. & Boles, B. R. (2010). The use of drip flow and rotating disk reactors for Staphylococcus aureus biofilm analysis. *Journal of visualized experiments : JoVE, 46*, e2470.

Schwartz, K., Syed, A. K., Stephenson, R. E., Rickard, A. H. & Boles, B. R. (2012). Functional amyloids composed of phenol soluble modulins stabilize Staphylococcus aureus biofilms. *PLoS pathogens, 8*(6), e1002744.

Scott, J. R. & Barnett, T. C. (2006). Surface proteins of gram-positive bacteria and how they get there. *Annual review of microbiology, 60*(1), 397-423.

Sevimli, F. & Yılmaz, A. (2012). Surface functionalization of SBA-15 particles for amoxicillin delivery. *Microporous and Mesoporous Materials 158:* 281-291.

Shafique, M., Alvi, I. A., Abbas, Z. & Rehman, S. (2017). Assessment of biofilm removal capacity of a broad host range bacteriophage JHP against Pseudomonas aeruginosa. *APMIS : acta pathologica, microbiologica et immunologica Scandinavica, 125*(6), 579-584.

Singh, P. (2016). SPR Biosensors: Historical Perspectives and Current Challenges. *Sensors and actuators. B, Chemical, 229*, 110-130.

Singla, S., Harjai, K. & Chhibber, S. (2013). Susceptibility of different phases of biofilm of Klebsiella pneumoniae to three different antibiotics. *Journal of antibiotics*, 66(2), 61-66.

Slomberg, D. L., Lu, Y., Broadnax, A. D., Hunter, R. A., Carpenter, A. W. & Schoenfisch, M. H. (2013). Role of Size and Shape on Biofilm Eradication for Nitric Oxide-Releasing Silica Nanoparticles. *ACS applied materials & interfaces, 5*(19), 9322-9329.

Slowing, I. I., Trewyn, B. G., Giri, S. & Lin, V. S.-Y. (2007). Mesoporous Silica Nanoparticles for Drug Delivery and Biosensing Applications. *Advanced Functional Materials 17*(8):1225-1236.

Slowing, I. I., Wu, C-W., Vivero-Escoto, J. L. & Lin, V. S.-Y. (2009). Mesoporous Silica Nanoparticles for Reducing Hemolytic Activity Towards Mammalian Red Blood Cells. *Small 5*(1): 57-62.

Son, M. J. & Lee, S. (2021). Antibacterial toxicity of mesoporous silica nanoparticles with functional decoration of specific organic moieties. *Colloids and surfaces. A, Physicochemical and engineering aspects, 630*, 127612.

Sperandio, V., Torres, A. G. & Kaper, J. B. (2002). Quorum sensing Escherichia coli regulators B and C (QseBC): A novel two-component regulatory system

involved in the regulation of flagella and motility by quorum sensing in E. coli. *Molecular microbiology, 43*(3), 809-821.

Stepanovic, S., Vukovic, D., Hola, V., Bonaventura, G.D., Djukic, S., Cirkovic, I, & Ruzicka, F. (2007). Quantification of biofilm in microtiter plates: Overview of testing conditions and practical recommendations for assessment of biofilm production by staphylococci. *APMIS : acta pathologica, microbiologica et immunologica Scandinavica, 115*(8), 891-899.

Stewart, P. S. (1996). Theoretical aspects of antibiotic diffusion into microbial biofilms. *Antimicrobial Agents and Chemotherapy, 40*(11), 2517-2522.

Stewart, P. S. & Franklin, M. J. (2008). Physiological heterogeneity in biofilms. *Nature Reviews Microbiology* 6(3): 199.

Stoodley, P., Debeer, D. & Lewandowski, Z. (1994). Liquid Flow in Biofilm Systems. *Applied and Environmental Microbiology, 60*(8), 2711-2716.

Su Y., Fang Y. & Li T. (2021). Chapter One - Surface plasmon resonance sensing in cell biology and drug discovery. In Chen, Y. & Ma, T (Ed.), *Surface Plasmon Resonance in Bioanalysis* (Volume 95, p. 1-53). Elsevier.

Subramanian, A., Irudayaraj, J. & Ryan, T. (2006). Mono and dithiol surfaces on surface plasmon resonance biosensors for detection of Staphylococcus aureus. *Sensors and actuators. B, Chemical, 114*(1), 192-198.

Sutherland, I. W. (2001). Biofilm exopolysaccharides: A strong and sticky framework. *Microbiology (Society for General Microbiology), 147*(Pt 1), 3-9.

Taglialegna, A., Navarro, S., Ventura, S., Garnett, J. A., Matthews, S., Penades, J. R., Lasa, I., & Valle, J. (2016). Staphylococcal BAP proteins build amyloid scaffold biofilm matrices in response to environmental signals. *PLOS Pathogens*, *12*(6) 1-34.

Tamanna, T., Landersdorfer, C. B., Ng, H. J., Bulitta, J. B., Wood, P. & Yu, A. (2018). Prolonged and continuous antibacterial and anti-biofilm activities of thin films embedded with gentamicin-loaded mesoporous silica nanoparticles. *Applied nanoscience, 8*(6), 1471-1482.

Tang, F., Li, L. & Chen, D. (2012). Mesoporous Silica Nanoparticles: Synthesis, Biocompatibility and Drug Delivery. *Advanced Materials 24*(12): 1504-1534.

Tasia, W., Lei, C., Cao, Y., Ye, Q., He, Y. & Xu, C. (2020). Enhanced eradication of bacterial biofilms with DNase I-loaded silver-doped mesoporous silica nanoparticles. *Nanoscale, 12*(4), 2328-2332.

Taylor, A.D., Ladd, J., Homola, J. & Jiang S. (2008). Surface Plasmon Resonance for the Detection of Bacterial (SPR) Sensors Pathogens. In Zourob, M., Elwary, S. & Turner, A.: *Principles of Bacterial Detection: Biosensors, Recognition*

Receptors and Microsystems. Springer New York, 2008. http://ebookcentral.proquest.com/lib/abo-ebooks/detail.action?docID=364415

Teodósio, J., Simões, M., Melo, L. & Mergulhão, F. (2011). Flow cell hydrodynamics and their effects on E. coli biofilm formation under different nutrient conditions and turbulent flow. *Biofouling (Chur, Switzerland), 27*(1), 1-11.

Toledo-Arana, A., Valle, J., Solano, C., Arrizubieta María Jesús, Cucarella, C., Lamata, M., Amorena, B., Leiva José, Penadés José Rafael, & Lasa Iñigo. (2001). The enterococcal surface protein, ESP, is involved in enterococcus faecalis biofilm formation. *Applied and Environmental Microbiology*, *67*(10), 4538–4545.

Trotonda, M. P., Manna, A. C., Cheung, A. L., Lasa I., & Penadés José R. (2005). Sara positively controls BAP-dependent biofilm formation in Staphylococcus aureus. *Journal of Bacteriology*, *187*(16), 5790–5798.

Vallet-Regí, M. (2006). Ordered Mesoporous Materials in the Context of Drug Delivery Systems and Bone Tissue Engineering. *Chemistry: a European journal,* 12(23), 5934-5943.

Verma, N., Srivastava, S., Malik, R., Goyal, P. & Pandey, J. (2022) Inhibition and disintegration of Bacillus subtilis biofilm with small molecule inhibitors identified through virtual screening for targeting TasA(28-261), the major protein component of ECM. *Journal of biomolecular structure & dynamics, ahead-of-print*(ahead-of-print), 1-17.

Wahlen, L., Mantei, J. R., DiOrio, J. P., Jones, C. M. & Pasmore, M. E. (2018). Production and analysis of a Bacillus subtilis biofilm comprised of vegetative cells and spores using a modified colony biofilm model. *Journal of microbiological methods, 148*, 181-187.

Walter, J., Chagnaud, P., Tannock, G. W., Loach, D. M., Dal Bello, F., Jenkinson, H. F., Hammes, W. P., & Hertel, C. (2005). A high-molecular-mass surface protein (LSP) and methionine sulfoxide reductase B (MSRB) contribute to the ecological performance of *lactobacillus reuteri* in the murine gut. *Applied and Environmental Microbiology*, *71*(2), 979–986.

Wang, H., Van Der Voort, P., Qu, H. & Liu, S. (2013). A simple room-temperature synthesis of mesoporous silica rods with tunable size and porosity. *Journal of nanoparticle research : an interdisciplinary forum for nanoscale science and technology, 15*(3), 1-8.

Wang, J., Song, M., Pan, J., Shen, X., Liu, W., Zhang, X., Li, H., & Deng, X. (2018). Quercetin impairs streptococcus pneumoniae biofilm formation by inhibiting

sortase A activity. *Journal of Cellular and Molecular Medicine*, *22*(12), 6228–6237.

Wang, X., Preston, J. F., III., & Romeo, T. (2004). The pgaABCD Locus of Escherichia coli Promotes the Synthesis of a Polysaccharide Adhesin Required for Biofilm Formation. *Journal of Bacteriology, 186*(9), 2724-2734.

Waters, C. M. & Bassler, B. L. (2005). Quorum sensing: Cell-to-cell communication in bacteria. *Annual review of cell and developmental biology, 21*(1), 319-346.

Whitchurch, C. B., Tolker-Nielsen, T., Ragas, P. C. & Mattick, J. S. (2002). Extracellular DNA Required for Bacterial Biofilm Formation. *Science (American Association for the Advancement of Science), 295*(5559), 1487.

Woods, P. W., Haynes, Z. M., Mina, E. G. & Marques, C. N. H. (2018). Maintenance of S. aureus in Co-culture With P. aeruginosa While Growing as Biofilms. *Frontiers in microbiology, 9*, 3291.

World Health Organization (2018*), Antibiotic resistance* [Electronic resource]. Retrieved from https://www.who.int/news-room/fact-sheets/detail/antibiotic-resistance (10.02.2019)

Wright, K. J., Seed, P. C. & Hultgren, S. J. (2007). Development of intracellular bacterial communities of uropathogenic Escherichia coli depends on type 1 pili. *Cellular microbiology, 9*(9), 2230-2241.

Wu, H., Song, Z., Hentzer, M., Andersen, J. B., Molin, S., Givskov, M. & Høiby, N. (2004). Synthetic furanones inhibit quorum-sensing and enhance bacterial clearance in Pseudomonas aeruginosa lung infection in mice. *Journal of antimicrobial chemotherapy, 53*(6), 1054-1061.

Wu, J., Li, F., Hu, X., Lu, J., Sun, X., Gao, J. & Ling, D. (2019). Responsive Assembly of Silver Nanoclusters with a Biofilm Locally Amplified Bactericidal Effect to Enhance Treatments against Multi-Drug-Resistant Bacterial Infections. *ACS central science, 5*(8), p. 1366

Wu, S. H., Mou, C. Y., & Lin, H. P. (2013). Synthesis of mesoporous silica nanoparticles. *Chemical Society Reviews 42*(9): 3862-3875.

Yasuda, H., Koga, T. & Fukuoka, T. (1999). [43] In vitro and in Vivo models of bacterial biofilms. *Methods in Enzymology*, 310, 577-595.

Zhang, J., Wang, H., Xie, T., Huang, Q., Xiong, X., Liu, Q. & Wang, G. (2020). The YmdB protein regulates biofilm formation dependent on the repressor SinR in Bacillus cereus 0–9. *World journal of microbiology & biotechnology, 36*(11), 165.

Zhang, P., Guo, J.-S., Yan, P., Chen, Y.-P., Wang, W., Dai, Y.-Z., Fang, F., Wang, G.-X., & Shen, Y. (2018). Dynamic dispersal of surface layer biofilm induced by

nanosized TiO2 based on surface plasmon resonance and waveguide. *Applied and Environmental Microbiology, 84*(9).

Zhang, W., Sileika, T. S., Chen, C., Liu, Y., Lee, J. & Packman, A. I. (2011). A novel planar flow cell for studies of biofilm heterogeneity and flow-biofilm interactions. *Biotechnology and bioengineering, 108*(11), 2571-2582.

Zhang, X., Bishop, P. & Kupferle, M. (1998). Measurement of polysaccharides and proteins in biofilm extracellular polymers. *Water science and technology, 37*(4-5), 345-348.

Zhao, Y., Wang, Y., Ran, F., Cui, Y., Liu, C., Zhao, Q., Gao, Y. & Wang, S. (2017). A comparison between sphere and rod nanoparticles regarding their in vivo biological behavior and pharmacokinetics. *Scientific reports*, 7(1), 4131-11.

Zhou, Y., Quan, G., Wu, Q., Zhang, X., Niu, B., Wu, B., Huang, Y., Pan, X. & Wu, C. (2018). Mesoporous silica nanoparticles for drug and gene delivery. *Acta Pharmaceutica Sinica B*, 8(2), pp.165-177.

Zogaj, X., Nimtz, M., Rohde, M., Bokranz, W. & Römling, U. (2001). The multicellular morphotypes of Salmonella typhimurium and Escherichia coli produce cellulose as the second component of the extracellular matrix. *Molecular microbiology, 39*(6), 1452-1463.